Title

Characterization of Putative Factors Involved in CO2-mediated Stomatal Signaling in Arabidopsis thaliana

Permalink

https://escholarship.org/uc/item/6ck8c2qf

Author

Chinn, Logan Brent

Publication Date

2022

Peer reviewed|Thesis/dissertation

UNIVERSITY OF CALIFORNIA SAN DIEGO

Characterization of Putative Factors Involved in CO_2-mediated

Stomatal Signaling in *Arabidopsis thaliana*

A thesis submitted in partial satisfaction of the requirements for the degree Master of Science

in

Biology

by

Logan Brent Chinn

Committee in charge:

Professor Julian Schroeder, Chair
Professor Martin Yanofsky
Professor Yunde Zhao

2022

The thesis of Logan Brent Chinn is approved, and it is acceptable in quality and form for publication on microfilm and electronically.

University of California San Diego

2022

TABLE OF CONTENTS

LIST OF FIGURES

LIST OF TABLES

ACKNOWLEDGEMENTS

Thank you to Dr. Julian Schroeder for your encouragement, knowledge, and the opportunity to conduct research and learn in your laboratory. Thank you to my other committee members Drs. Yunde Zhao and Marty Yanofsky.

Thank you to my immediate mentors Guillaume Dubeaux and Kelsey Swink for your assistance, patience, and introduction to this project. I would also like to thank Katie Lu, Karnelia Paul, and Sabrina Lin for their support in this project.

Lastly, thank you to my family and friends for your constant support throughout this chapter in my life.

ABSTRACT OF THE THESIS

Characterization of Putative Factors Involved in CO_2-mediated

Stomatal Signaling in *Arabidopsis thaliana*

by

Logan Brent Chinn

Master of Science in Biology

University of California San Diego, 2022

Professor Julian Schroeder, Chair

With atmospheric CO_2 levels steadily increasing, it is important for humans to understand

how plants utilize CO_2 and release O_2 in the air we breathe. Several CO_2 signaling components

have been characterized, but there are still many unknown components of the CO_2 signaling

pathway. This thesis characterizes candidate mutant plants from a comprehensive artificial

microRNA (amiRNA) forward genetic screen designed to isolate putative mutants involved in

CO$_2$ signaling. Each mutant carried an amiRNA specifically designed to downregulate a few genes in *Arabidopsis thaliana.* 39 putative mutants were isolated and confirmed at the T3 generation. This project aims to elucidate the role of these genes in CO$_2$-mediated stomatal responses and stomatal development. Gas exchange assays under defined changes in CO$_2$ concentrations were performed to quantify the stomatal conductance and kinetic responses of the candidates. Stomatal density assays were performed to quantify the number of stomata of the candidates. The database ePlant and a Python script were utilized to determine potential interactions between the targeted amiRNA loci and known CO$_2$-mediated stomatal signaling components. The results highlight 15 candidate mutants with unique responses to imposed shifts in CO$_2$ concentration and varying stomatal densities compared to HsMYO (wild-type control) plants. 6 of the putative mutants show an inhibited response to defined changes in CO$_2$ concentration or are affected in stomatal development and warrant further investigation. The 6 putative mutants have been retransformed in wild-type plants and will be examined to verify the robustness of the mutant phenotypes seen in this thesis.

1. INTRODUCTION

Plants have a vital relationship with humans; as plants conduct photosynthesis, they utilize carbon dioxide (CO_2) to produce energy, and in return release water vapor and oxygen (O_2). Inversely, humans respire CO_2 as they breathe in O_2, thereby completing the cycle. These important molecules enter as well as leave plants through stomata, which are pores found on nearly all species of land plants. Every stoma is bordered by a pair of guard cells which can physically change the size of stomata, allowing plants to respond to different environmental changes including fluctuating levels of atmospheric CO_2 and light (Engineer et al., 2016). Atmospheric CO_2 affects plant intercellular carbon (C_i) levels which help plants sense whether to open or close their stomata (Engineer et al., 2016). Low C_i levels will cause stomata to open wider, while high C_i levels will cause stomata to close.

Importantly, atmospheric levels of CO_2 have been steadily rising since the start of the industrial revolution, mostly due to humans burning fossil fuels and releasing an excess of CO_2 molecules into the atmosphere (Höök & Tang, 2013). The Keeling Curve, which is a data record of the daily level of CO_2 concentration since 1958, estimates that average global CO_2 levels have risen over 100 ppm in the past 50 years (Keeling et al., 1976, Howe, 2015). As a result, stomata have been narrowing their central gas exchange pores globally, resulting in a decrease in stomatal conductance, or the degree of a stomatal opening (Zhang et al., 2018). Reductions in stomatal conductance have mixed effects in plants; water loss is diminished but crop yields are also reduced (Keenan et al., 2013). Consequently, it is imperative to fully understand CO_2 signaling to generate crop plants which can efficiently balance water use with excess atmospheric CO_2.

1

Arabidopsis thaliana is used as a model organism in land plant studies because it has a short flowering and reproduction time compared to many other plants, allowing for efficient experimental timelines (Koornneef & Meinke, 2010). Additionally, *A. thaliana* has a relatively small genome compared to most plants and was the first full plant genome to be sequenced, making gene identification relatively straightforward in mutant plants (*The Arabidopsis Genome Initiative*).

The CO_2 signaling pathway in the guard cells of plants is the sensory system in which plants can respond to changing levels of environmental CO_2 through a cascade of activated and inhibited genes (Zhang et al., 2018). Many studies in this niche have focused on the characterization of one or two genes, how those genes interact with the rest of the CO_2 signaling pathway, and the effect on stomata when those genes are disrupted. In the past 20 years, many new genes have been implicated in the CO_2 signaling pathway. First, βCA1 and βCA4 are upstream carbonic anhydrases vital in the CO_2 signaling pathway as they convert incoming CO_2 into bicarbonate and protons (Hu et al., 2015). Bicarbonate is essential in activating downstream CO_2 signaling pathway components, so when βCA1 and βCA4 are silenced, stomata take longer to respond to changes in CO_2 levels (Engineer et al., 2016). Similarly, rice has comparable delays in stomatal response when its own carbonic anhydrase is disrupted, demonstrating these carbonic anhydrases remain important in crop plants (Chen et al., 2017). Importantly, high C_i levels will lead to an excess of intracellular bicarbonate ions, activating SLAC1 anion channels. SLAC1 anion channels will increase chloride and malate anions movement across the guard cell plasma membrane and cause stomata to close (Negi et al., 2008).

Other genes implicated in plant CO_2 signaling pathway include MPK4 and MPK12, which are mitogen-activated protein kinases that have been found to respond to CO_2, but not

abscisic acid (ABA), a plant hormone created from abiotic stresses which induces stomatal closure (Jakobson et al., 2016; Marten et al., 2008). HT1 is another protein kinase which negatively regulates stomatal closure, so disruption of this gene will cause impaired stomatal response to changes in CO_2 concentration (Hashimoto et al., 2006). Further, CBC1 and CBC2 are in the same family of kinases and both exhibit an impaired response to CO_2 and blue light when mutated (Hiyama et al., 2017). Importantly, MPK4 and MPK12 inhibit activity of HT1, while HT1 is likely to interact with CBC1 and CBC2 (Hiyama et al., 2017; Hõrak et al., 2016). Finally, OST1 is a protein kinase which affects stomatal movements, with mutants of this protein showing impaired stomatal closure (Xue et al., 2011). Recently, elevated CO_2 were shown to not increase activity of OST1, suggesting basal expression levels of OST1 are adequate to accelerate CO_2 response (Hsu et al., 2018; Zhang et al., 2020). In all, around 20 genes have been discovered in the CO_2 signaling pathway and many of the genes are predicted to interact with one another, but there are still holes in the transduction network. There are multiple unidentified genes within the pathway that have yet to be characterized. Notably, it is still unknown how plants sense bicarbonate to activate downstream signaling components. Moreover, the interaction mechanisms of many currently known genes have yet to be discovered.

One of the difficulties studying plant signaling pathways relates to the fact that plants often have extremely large gene families with redundant function, requiring multiple gene knockouts to obtain a strong phenotype. Consequently, single gene knockouts in *A. thaliana* will oftentimes only result in very mild phenotypes, so researchers have developed strategies to create higher order mutants (Park et al., 2009). An artificial microRNA (amiRNA) screen is an effective tool to isolate possible genes or gene families as researchers can use premade amiRNA libraries to test thousands of plants with multiple mutated genes in a short period of time (Hauser

et al., 2013). An amiRNA is computationally designed and binds to partially complementary mRNAs to silence protein translation (Schwab., et al 2006). Additionally, as amiRNAs target multiple closely related genes, amiRNA screens can isolate functionally redundant proteins (Hauser et al., 2019). In this study, I aim to characterize new genes that may be involved in the CO_2 signaling pathway in plants from a previously conducted forward genetic amiRNA screen (Swink, K. 2021). Additionally, through published datasets, I plan to generate predictive networks of gene functions and associations by connecting the newly identified genes with existing omics networks such as interactomes and transcriptomes.

In the previously conducted amiRNA forward genetic screen, Col0 (wild type) plants were transformed with a genome-wide library of amiRNAs to isolate new genetic mutants which affect the response of *Arabidopsis thaliana* to varying CO_2 concentration (Hauser et al., 2013). Initial candidate plants were isolated through low CO_2 treatment (150 ppm for 2 hours) and immediate subsequent infrared thermal imaging to find plants which had hotter leaves than the rest of the population. Plants unable to respond properly to CO_2 had narrower stomata even after low CO_2 concentration treatment, resulting in less water vapor exiting stomata and consequently hotter leaves. 75 putative candidates were isolated from the primary screen. Seeds of these candidates were then harvested, and a secondary confirmation screen was conducted in the following T3 generation with the same conditions as the primary screen. After the secondary screen, 39 putative candidates were confirmed. From these 39 candidates, 26 candidates remained after amiRNA sequencing confirmation and literature review.

In this thesis, I present preliminary data on 15 of these candidates. Through my experiments of these putative candidates, I found seven candidate mutants to display reduced stomatal response to changes in atmospheric CO_2 levels compared to wild type. I have also

isolated multiple stomatal developmental mutants, which involve genes that play a role in the formation of stomata rather than affect stomatal response. These preliminary data show a reduced stomatal density and a fully shifted stomatal conductance curve but require further trials. Through bioinformatic analysis, I have also found possible links between candidate genes and known CO_2 signaling components and generated predictive interactome networks. From the stomatal conductance data, stomatal density data, and interactome networks, six of these putative candidates were chosen to be studied further in future experiments. Overall, my experimental data reveals multiple genes possibly implicated in CO_2-mediated stomatal response and may eventually result in the development of more efficient food crops in terms of CO_2 and water use.

2. RESULTS

An amiRNA screen was pursued to identify new genetic mutants that impair the response of *Arabidopsis thaliana* to shifts in CO_2 concentration. A database with over 2 million amiRNAs (phantomdb.ucsd.edu) was utilized to create an amiRNA library of 22,000 amiRNAs. This library generated approximately 14,000 amiRNA plants in the T2 generation which were then screened using pools of 90 lines and 20 seeds per line by exposing 3-week-old plants to low CO_2 (150 ppm) for two hours (Hauser et al., 2019). amiRNA lines were grown alongside HsMYO plants as the wild-type control and High Leaf Temperature 1-2 (*ht1-2)* as the hot leaf temperature control, since the *ht1-2* mutant is known to not respond properly to low levels of CO_2 (Hashimoto et al., 2006).

75 putative mutants were isolated in the primary screen, based on the results of the infrared thermal imaging immediately after low CO_2 treatment and scoring of a higher leaf temperature (Swink, K. 2021). In a secondary confirmation screen, individual putative mutant lines (2 plants per pot) were grown alongside 1 HsMYO plant and 1 *ht1-2* plant. Plants were grown to 3-4 weeks and treated with low CO_2 (150 ppm) for two hours before infrared thermal imaging (Swink, K. 2021). 39 putative amiRNA candidate lines were isolated from the secondary rescreen and 26 lines remained after amiRNA sequencing confirmation and literature review. In the following results, I describe and characterize many of the individual amiRNA lines that were isolated and confirmed from the secondary infrared screen.

First, LC17, a candidate plant line with a predicted downregulated receptor-like protein kinase, had slightly hotter leaves on average than the wild-type control line (HsMYO) at ambient CO_2 conditions (Figure 1). HsMYO plants were used as the control for these experiments involving amiRNA lines as HsMYO plants have an inserted amiRNA targeting the human

6

myosin 2 gene and no targets in *A. thaliana* (Hauser et al., 2013). Importantly, this ensures the results observed for the mutant amiRNA lines are unlikely to have been from the amiRNA insertion process itself, but rather the downregulation of the predicted target proteins. Note that for the infrared thermal images shown in the present thesis, images were captured at ambient CO_2 (415 ppm), which differs from the original primary and secondary screens. Therefore, the temperature differences previously noted in the screens are not necessarily seen in the image data captured in my experiments that are shown here. Nevertheless, these images provide data on temperatures found at ambient CO_2 for comparison to those identified at low CO_2 (150 ppm) (Swink, K. 2021). LC17 plants and the control plants responded to changes in CO_2 (Figure 2). Both LC17 and control plants showed a highly increased stomatal conductance in response to low CO_2 treatment. Additionally, both plants showed a decreased stomatal conductance in response to high CO_2 treatment. Interestingly, LC17 plants had a statistically significant lower number of stomata ($p < .001$) compared to HsMYO plants, but this had no effect on stomatal conductance, even at ambient CO_2 levels (Figure 3). Further amiRNA candidate lines were investigated, as the phenotypes of line LC17 were not sufficiently pronounced for further characterization.

Figure 1: Bright-Field and Infrared Temperature Images of a Receptor-Like Protein Kinase Targeting amiRNA Line (LC17) and Control (HsMYO) Plants at Ambient [CO2].

Images of candidate and control plants highlighting the temperature of the plant leaves at ambient $[CO_2]$ - 415 ppm. Images are representative samples from 3–4-week plants of each plant line.
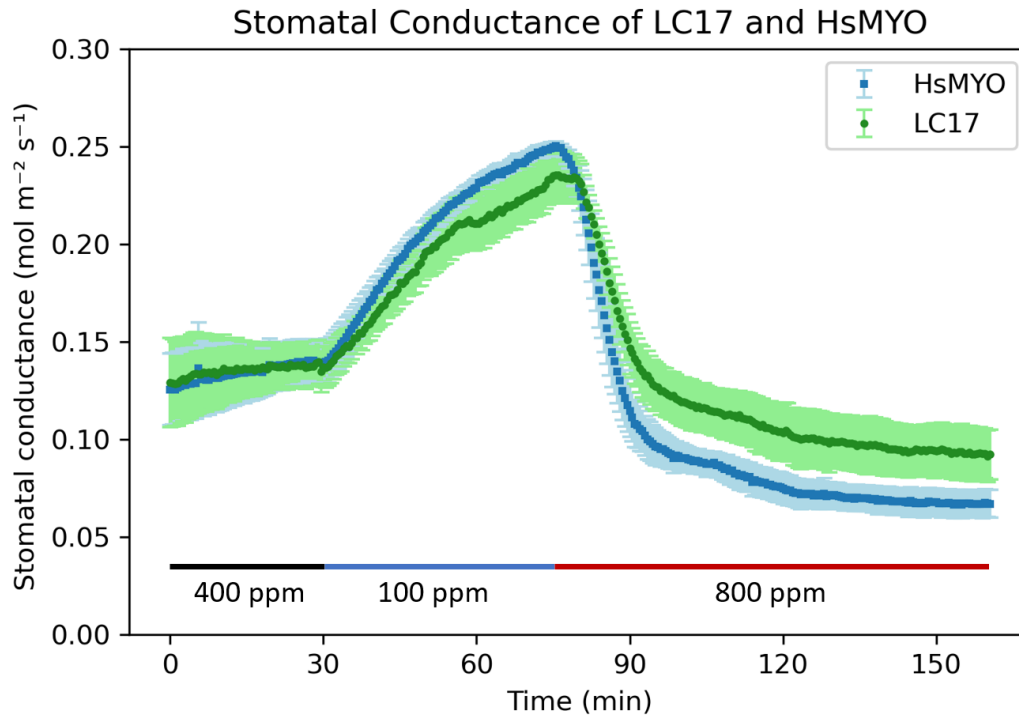
Figure 2: Stomatal Conductance of LC17 and HsMYO Plants in Response to Imposed Shifts in [CO2].

Time course assay of LC17 and HsMYO plant leaves in response to [CO_2]. Stomatal conductance was measured in leaves exposed to ambient CO_2 (400 ppm) for 30 minutes, low CO_2 (100 ppm) for 45 minutes, and high CO_2 (800 ppm) for 80 minutes. Stomatal conductance is a measurement of the rate of CO_2 entering or water vapor exiting the stomata; higher stomatal conductance indicates a larger stomatal opening. Data represent the mean ± SEM of three leaves from different 5–6-week-old plants.

Figure 3: Double-blinded Stomatal Density Assay of LC17 and HsMYO Plants.

Stomatal density assays comparing the average number of stomata between LC17 and HsMYO plants. A two-tailed t-test between the two groups yields a p-value < .001. The fifth true leaf of five different plants from each condition were harvested as samples. Five different images from each sample were taken via bright-field microscopy, totaling 25 images per genotype. The HsMYO data for all stomatal density assays is the same because all images were captured in the same experimental set.

LC22, a candidate plant line with predicted targets of silenced formin gene homologs, had hotter leaves on average compared to the control HsMYO plants at ambient CO_2 conditions (Figure 4). LC22 plants had a slightly lower stomatal conductance at ambient CO_2 conditions and a slower response to an imposed shift of low CO_2 compared to HsMYO plants (Figure 5A). Both LC22 and HsMYO plants responded to high concentrations of CO_2. The CO_2 variable gas exchange assay was performed twice with new samples for both genotypes and resulted in very

similar data (Figure 5B). The stomatal densities of LC22 and HsMYO plants were relatively

similar and did not have a statistically significant difference in number of stomata (Figure 6).
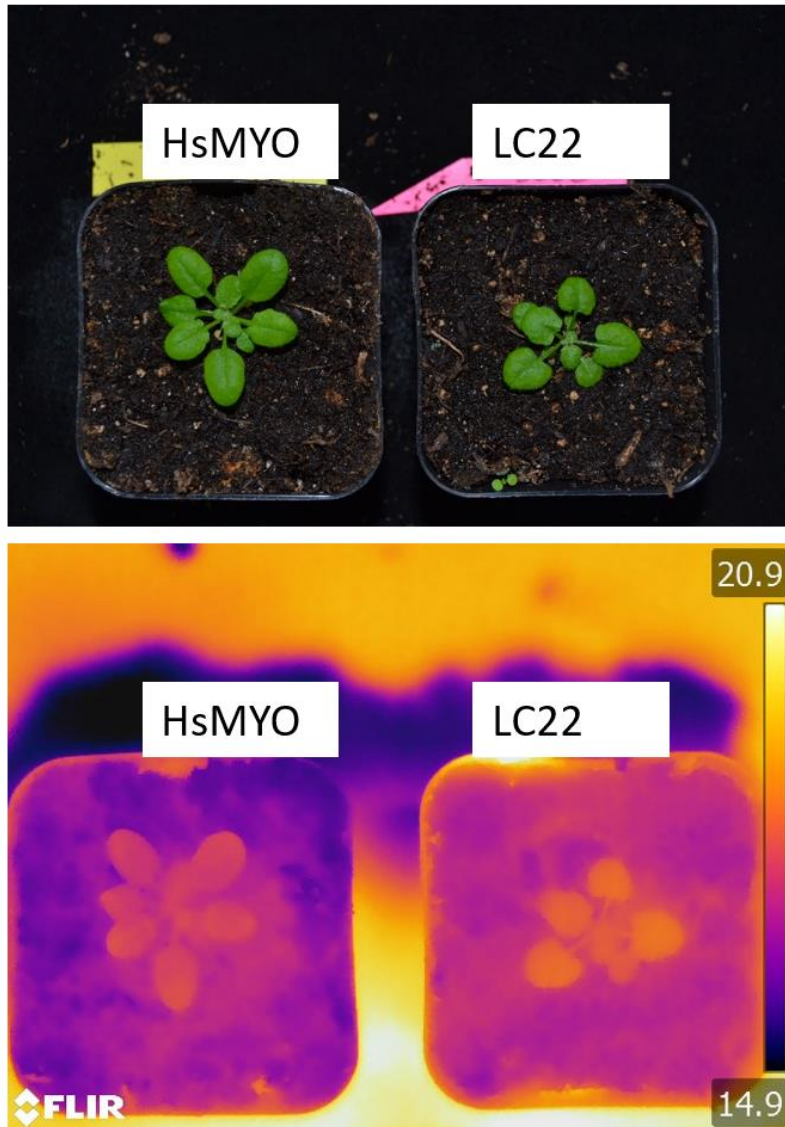
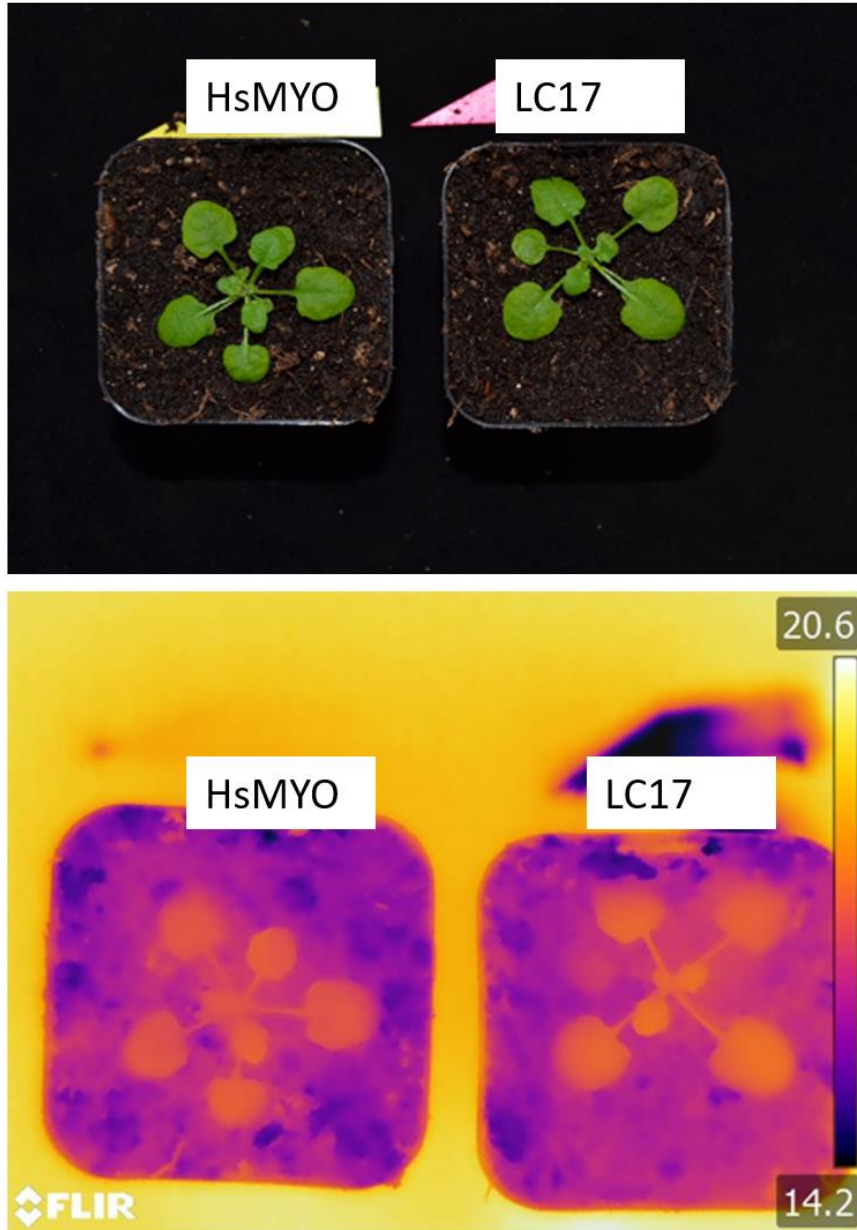**Figure 4: Bright-Field and Infrared Temperature Images of a Formin Homolog Targeting amiRNA Line (LC22) and Control (HsMYO) Plants at Ambient [CO2].**

Images of candidate and control plants highlighting the temperature of the plant leaves at ambient [CO_2] - 415 ppm. Images are representative samples from 3–4-week plants of each plant line.

Figure 5: Stomatal Conductance of LC22 and HsMYO Plants in Response to Imposed Shifts in [CO2].

Time course assay of LC22 and HsMYO plant leaves in response to [CO_2]. Stomatal conductance was measured in leaves exposed to ambient CO_2 (400 ppm) for 30 minutes, low CO_2 (100 ppm) for 45 minutes, and high CO_2 (800 ppm) for 80 minutes. Stomatal conductance is a measurement of the rate of CO_2 entering or water vapor exiting the stomata; higher stomatal conductance indicates a larger stomatal opening. Data represent the mean ± SEM of three leaves (5A) and four leaves (5B) from different 5–6-week-old plants.
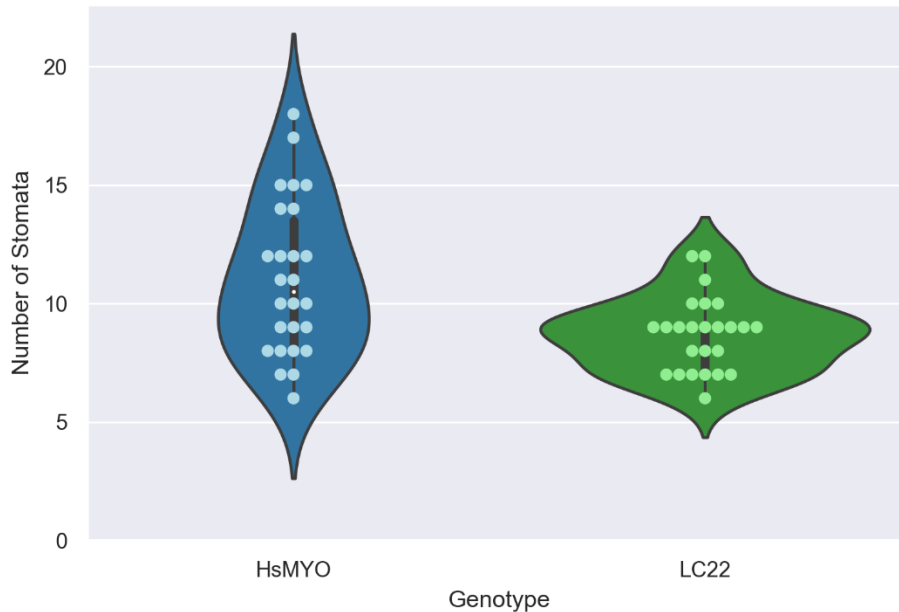
Figure 6: Double-blinded Stomatal Density Assay of LC22 and HsMYO Plants.
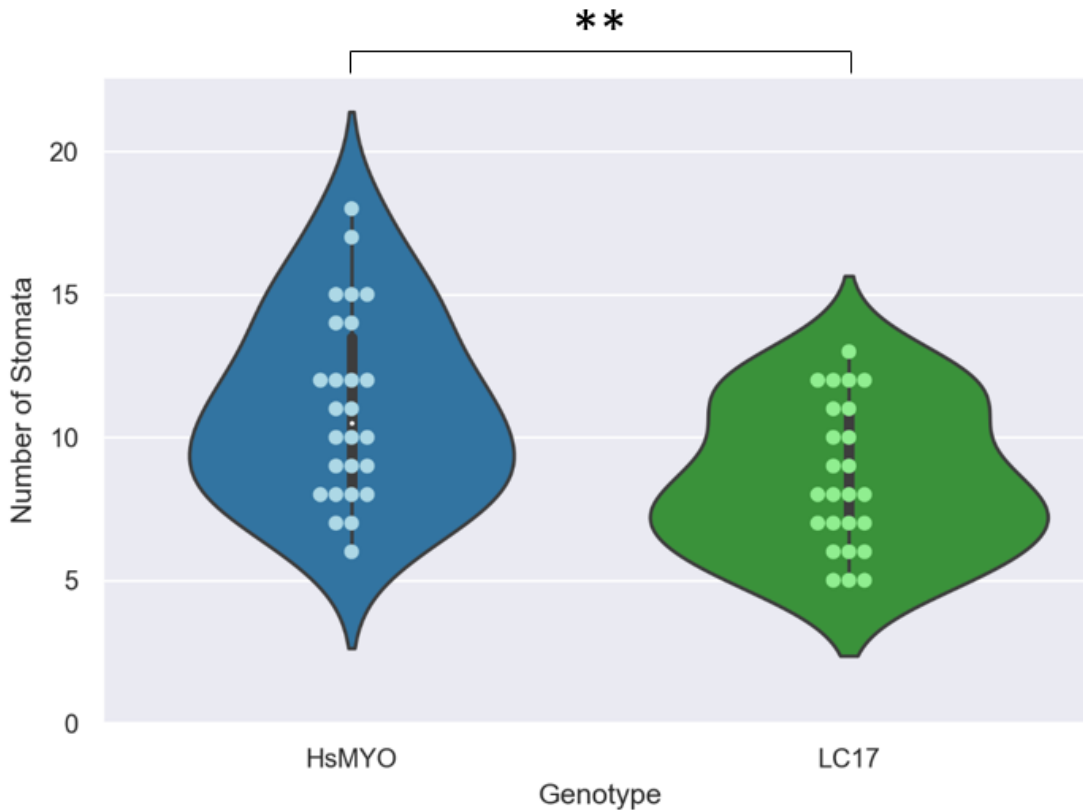
Stomatal density assays comparing the average number of stomata between LC22 and HsMYO plants. A two-tailed t-test between the two groups yields a p-value > .01. The fifth true leaf of five different plants from each condition were harvested as samples. Five different images from each sample were taken via bright-field microscopy, totaling 25 images per genotype. The HsMYO data for all stomatal density assays is the same because all images were captured in the same experimental set.

LC30 plants, a leucine-rich repeat protein targeting amiRNA line, had a statistically significant reduced number of stomata compared to the control (p < .0001, Figure 7). Further, the stomatal conductance of LC30 plants was much lower at ambient, low, and high concentrations of CO_2 relative to the control HsMYO plants (Figure 8A). However, when the LC30 data is normalized to the control stomatal conductance data, there was almost no difference between the genotypes, showing that the two plant lines responded to changes in CO_2 concentration (Figure 8B). Furthermore, screening led to isolation of multiple plants carrying the same amiRNA, LC27 and LC33, implicating a robust phenotype of this line (Swink, K. 2021). Bioinformatic data

mining suggests that one of the amiRNA targeted loci (AT3G43740) in LC30 plants has a predicted secondary interaction with known CO_2 signaling component Open Stomata 1 (OST1) through Diacylglycerol Kinase 2 (DGK2), a kinase involved in plant development and response to abiotic stress (Figure 9A). Interestingly these data together suggest that amiRNA line LC30 reduces stomatal density and thus causes the increased temperature found in primary and secondary screens for this line.
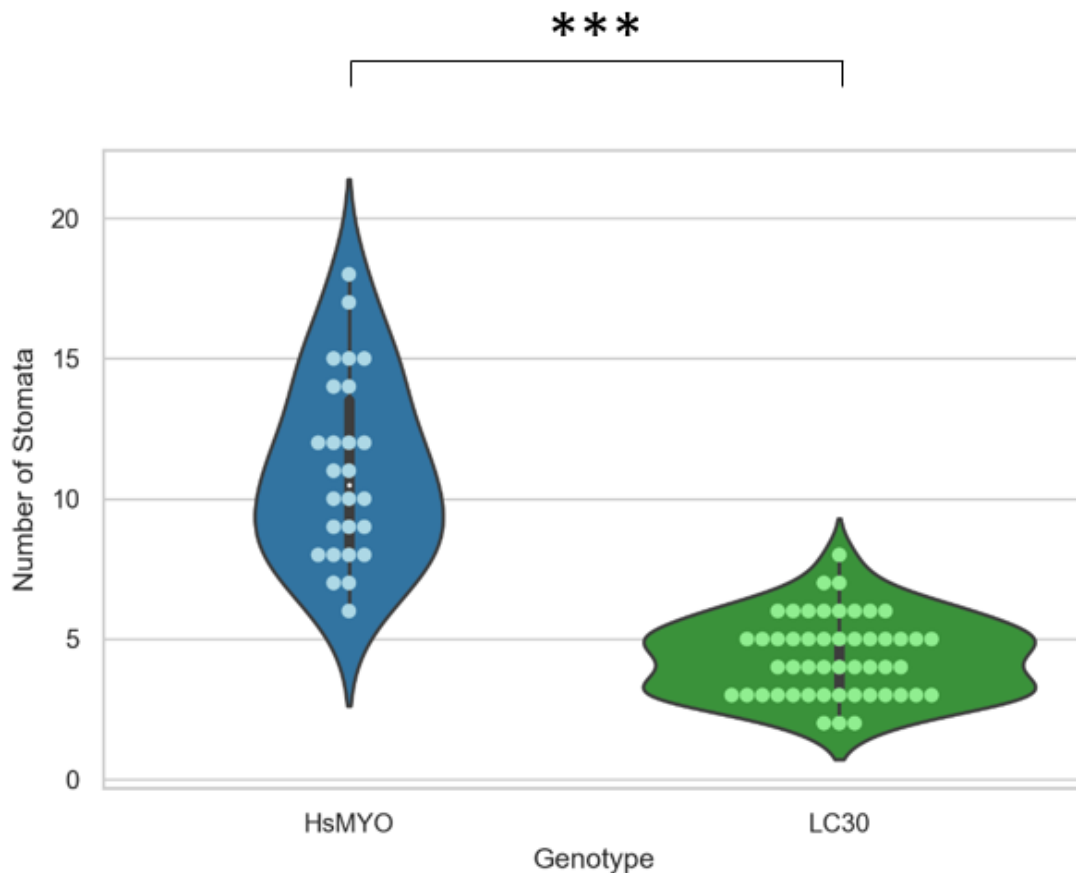
Figure 7: Double-blinded Stomatal Density Assay of a Leucine-rich Repeat Family Protein Targeting amiRNA Line (LC30) and Control (HsMYO) Plants.

Stomatal density assays comparing the average number of stomata between LC30 and HsMYO plants. A two-tailed t-test between the two groups yields a p-value < .0001. The fifth true leaf of five different plants from each condition were harvested as samples. Five different images from each sample were taken via bright-field microscopy, totaling 25 images per genotype. The HsMYO data for all stomatal density assays is the same because all images were captured in the same experimental set.
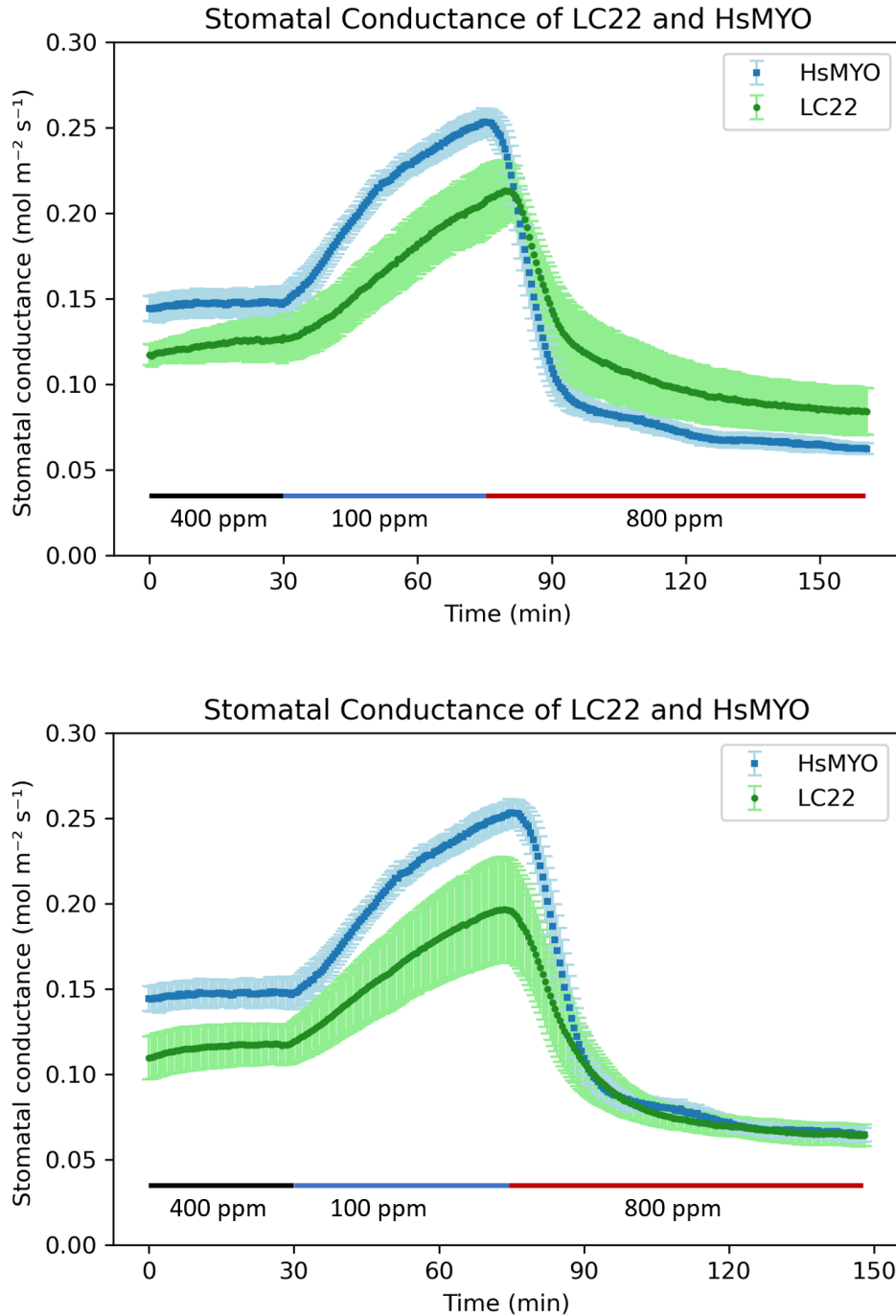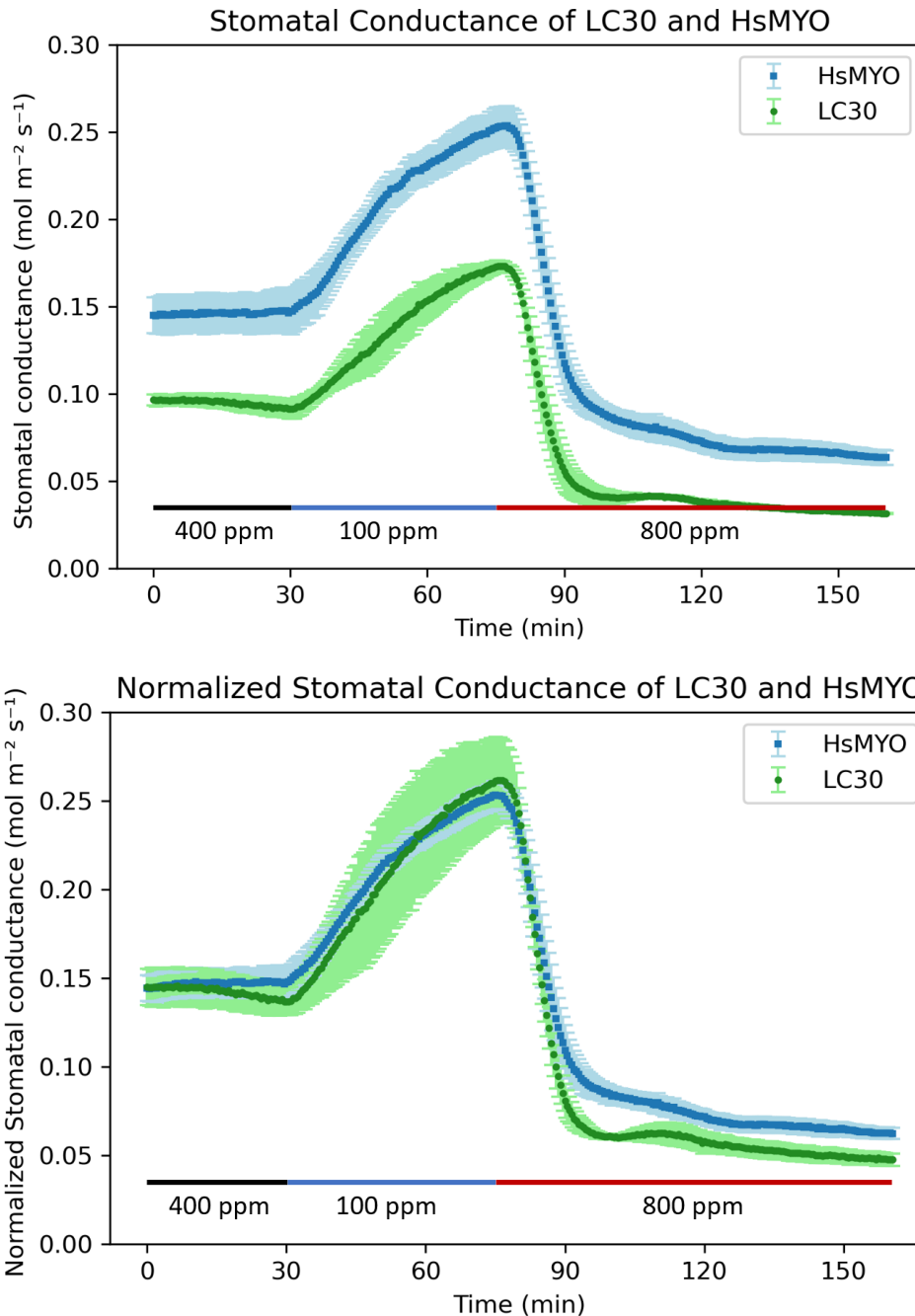
Figure 8: Stomatal Conductance of LC30 and HsMYO Plants in Response to Imposed Shifts in [CO2].

Time course assay of LC30 and HsMYO plant leaves in response to [CO_2]. Stomatal conductance was measured in leaves exposed to ambient CO_2 (400 ppm) for 30 minutes, low CO_2 (100 ppm) for 45 minutes, and high CO_2 (800 ppm) for 80 minutes. Figure 8B shows the stomatal conductance of LC30 plants normalized to HsMYO plants. Stomatal conductance is a measurement of the rate of CO_2 entering or water vapor exiting the stomata; higher stomatal conductance indicates a larger stomatal opening. Data represent the mean ± SEM of three leaves from different 5–6-week-old plants.

15
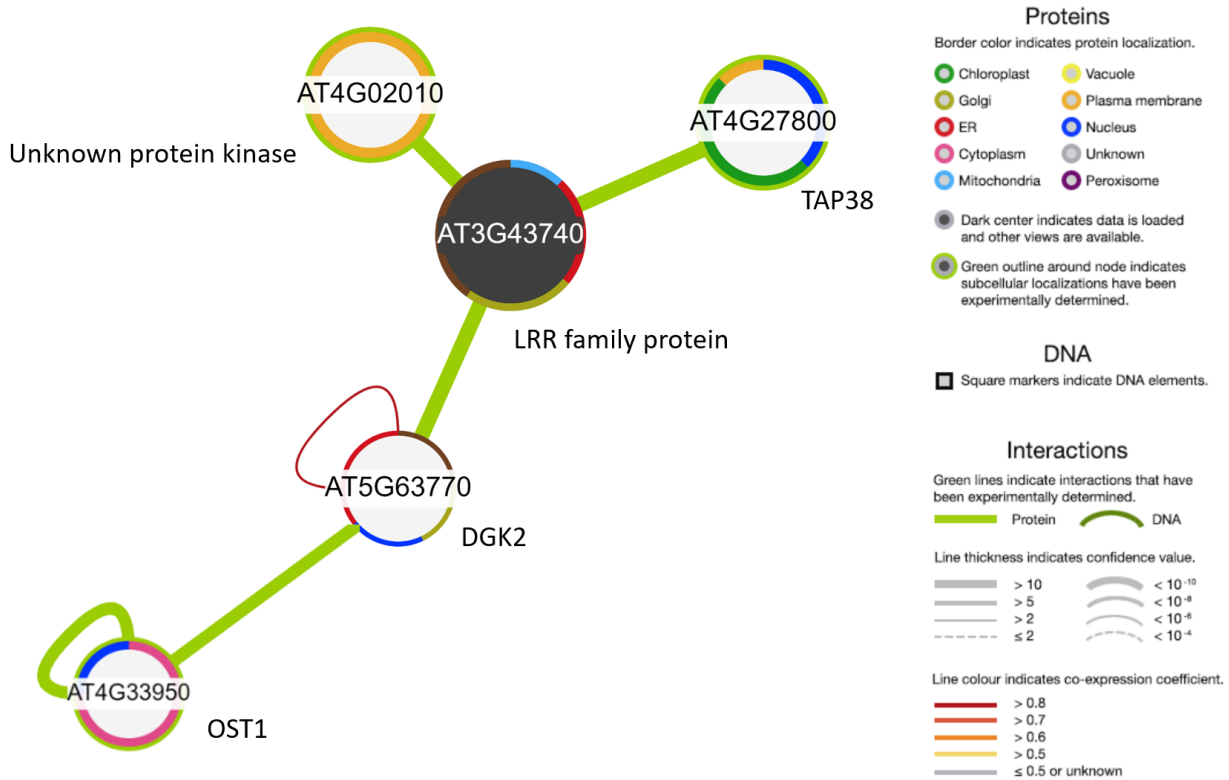
**Figure 9: Interactome of amiRNA Targeted Locus AT3G43740 in LC30.**

Interactome of a leucine-rich repeat family protein (locus AT3G43740) shown to interact with three proteins from published datasets: Thylakoid-associated phosphatase 38 (TAP38), Diacylglycerol kinase 2 (DGK2), and an unknown protein kinase as provided by the ePlant Interaction viewer (Waese et al., 2017). DGK2 is known to interact with OST1, a known component involved in CO2 signaling.

Meanwhile, LC28, a candidate plant line with downregulated nascent polypeptide-associated complex subunit alpha-like protein (NACA-like protein) homologs, displayed a highly affected response to changes in CO_2 compared to the control (Figure 10A). Firstly, LC28 plants had slightly lower stomatal conductance compared to the control at ambient CO_2 concentrations. While the control plants showed a highly increased stomatal conductance in response to low CO_2 treatment, LC28 plants had an inhibited response with stomatal conductance increasing only slightly. After high CO_2 treatment, control plants responded rapidly

by decreasing their stomatal conductance. However, LC28 plants had a slower initial response to high CO_2 treatment but eventually reached a similar stomatal conductance to control plants. The CO_2 variable gas exchange assay was performed twice with new samples for both genotypes and resulted in very similar data (Figure 10B). There was a statistically significant difference in stomatal densities between LC28 and HsMYO plants, which may have contributed to the lower stomatal conductance at ambient CO_2 (p < .01, Figure 11). Note however, that this stomatal density difference may mainly be due to some samples with higher stomatal densities in the HsMYO control (as described later in Figure 41 for an ANOVA analysis of the entire experimental set).
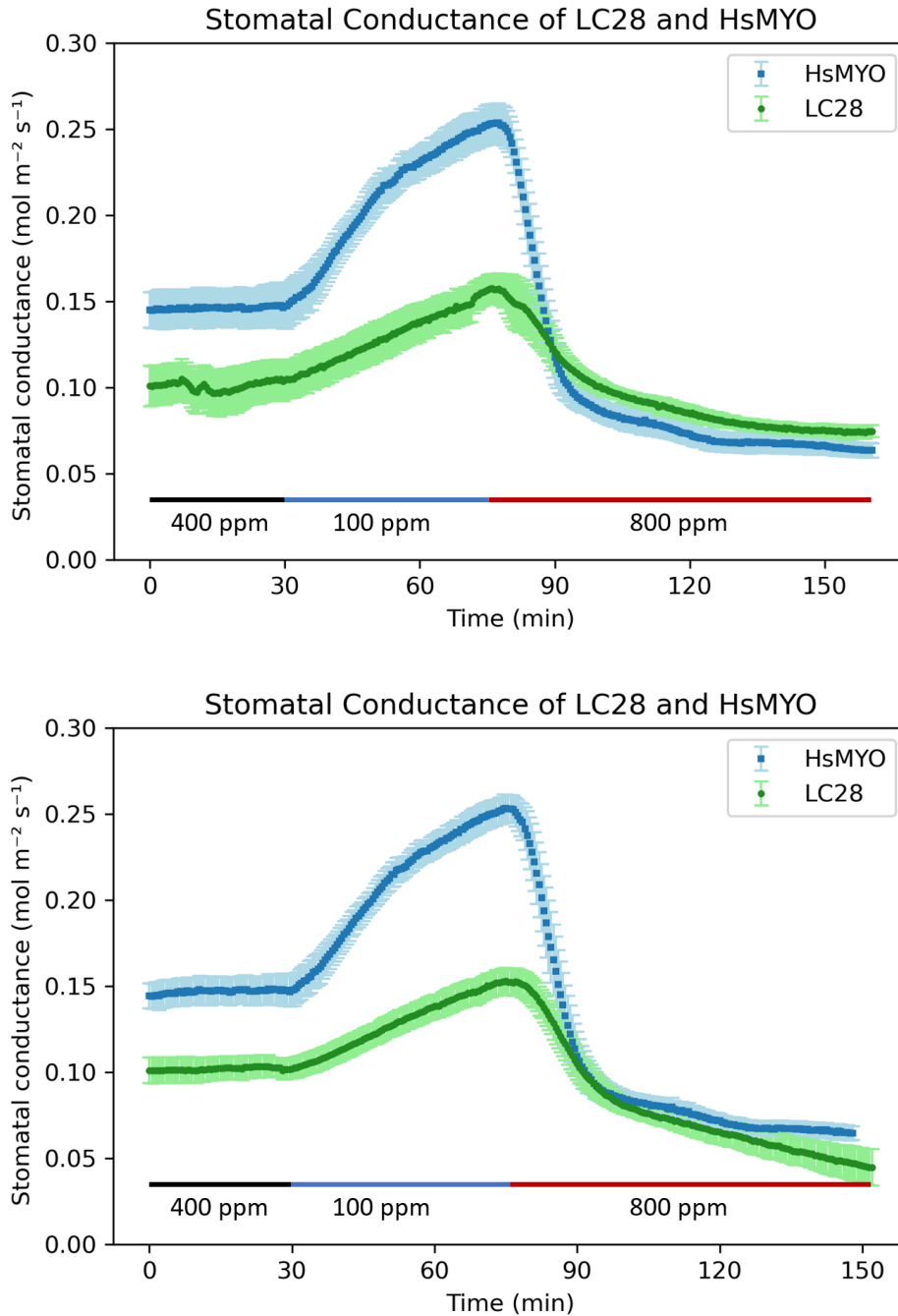
Figure 10: Stomatal Conductance of a Nascent Polypeptide-associated Complex Subunit Alpha-like Protein Targeting amiRNA Line (LC28) and Control (HsMYO) Plants in Response to Imposed Shifts in [CO2].

Time course assay of LC28 and HsMYO plant leaves in response to [CO_2]. Stomatal conductance was measured in leaves exposed to ambient CO_2 (400 ppm) for 30 minutes, low CO_2 (100 ppm) for 45 minutes, and high CO_2 (800 ppm) for 80 minutes. Stomatal conductance is a measurement of the rate of CO_2 entering or water vapor exiting the stomata; higher stomatal conductance indicates a larger stomatal opening. Data represent the mean ± SEM of three leaves (8A) and four leaves (8B) from different 5–6-week-old plants.

18

Figure 11: Double-blinded Stomatal Density Assay of LC28 and HsMYO Plants.

Stomatal density assays comparing the average number of stomata between LC28 and HsMYO plants. A two-tailed t-test between the two groups yields a p-value < .01. The fifth true leaf of five different plants from each condition were harvested as samples. Five different images from each sample were taken via bright-field microscopy, totaling 25 images per genotype. The HsMYO data for all stomatal density assays is the same because all images were captured in the same experimental set.

LC40 plant lines carry an amiRNA that was predicted to downregulate F-box protein homologs. LC40 plants had slightly cooler leaves on average compared to the wild-type control HsMYO plants at ambient CO_2 conditions (Figure 12). LC40 plants responded somewhat differently to changes in CO_2 concentration compared to HsMYO plants. At ambient CO_2 conditions, LC40 plants had a slightly reduced stomatal conductance comparted to control plants, but both plant lines responded to low CO_2 conditions (Figure 13). When exposed to high CO_2 concentrations, LC40 plants responded initially the same as control plants but did not decrease as

much in stomatal conductance after 120 minutes of high CO_2 treatment. The stomatal density

data reveals there was a statistically significant difference in the number of stomata between

LC40 and control plants, perhaps accounting for the lower stomatal conductance at ambient CO_2

($p < .01$, Figure 14).
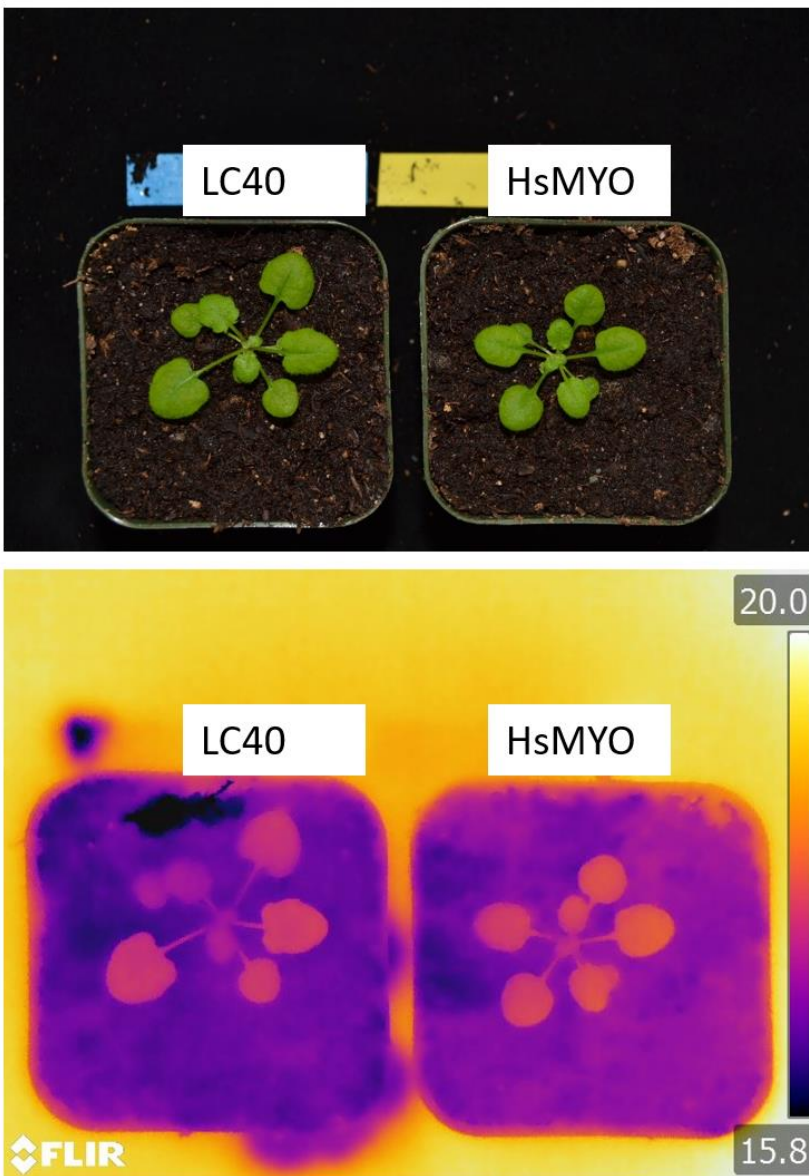
Figure 12: Bright-Field and Infrared Temperature Images of an F-box Protein Targeting amiRNA Line (LC40) and Control (HsMYO) Plants at Ambient [CO2].

Images of candidate and control plants highlighting the temperature of the plant leaves at ambient [CO_2] - 415 ppm. Images are representative samples from 3–4-week plants of each plant line.
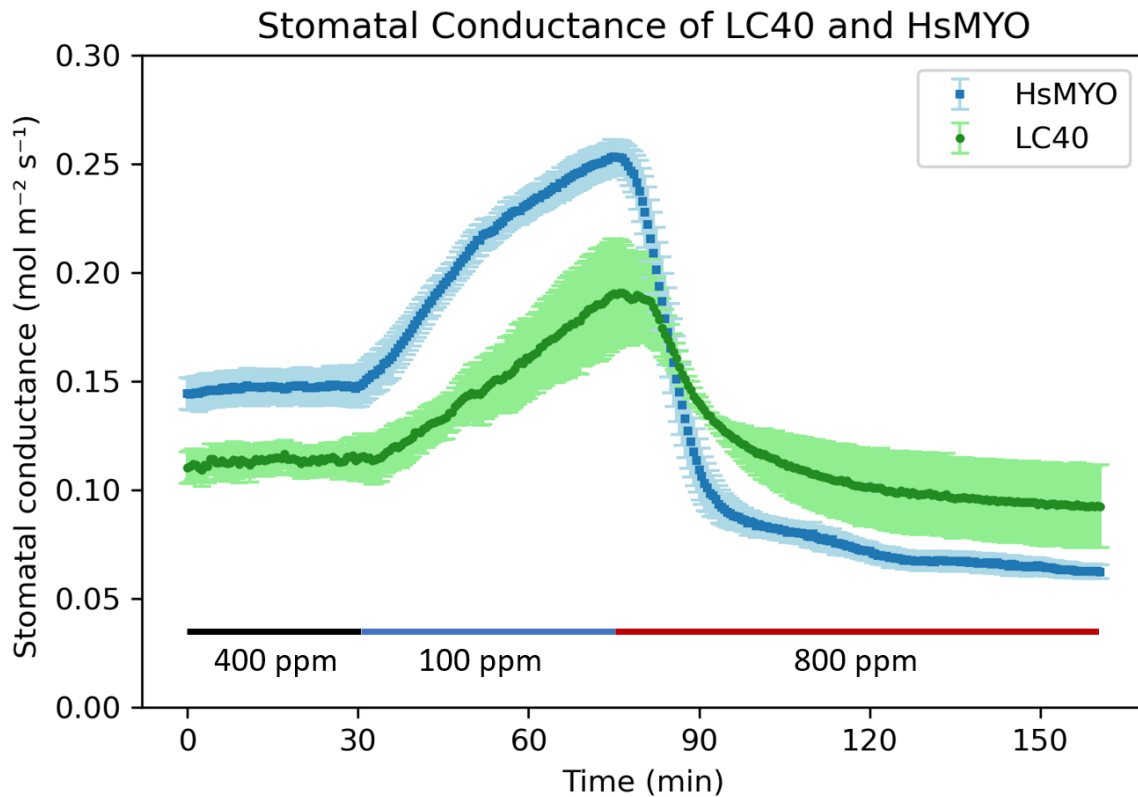
Figure 13: Stomatal Conductance of LC40 and HsMYO Plants in Response to Imposed Shifts in [CO2].

Time course assay of LC40 and HsMYO plant leaves in response to [CO_2]. Stomatal conductance was measured in leaves exposed to ambient CO_2 (400 ppm) for 30 minutes, low CO_2 (100 ppm) for 45 minutes, and high CO_2 (800 ppm) for 80 minutes. Stomatal conductance is a measurement of the rate of CO_2 entering or water vapor exiting the stomata; higher stomatal conductance indicates a larger stomatal opening. Data represent the mean ± SEM of three leaves from different 5–6-week-old plants.

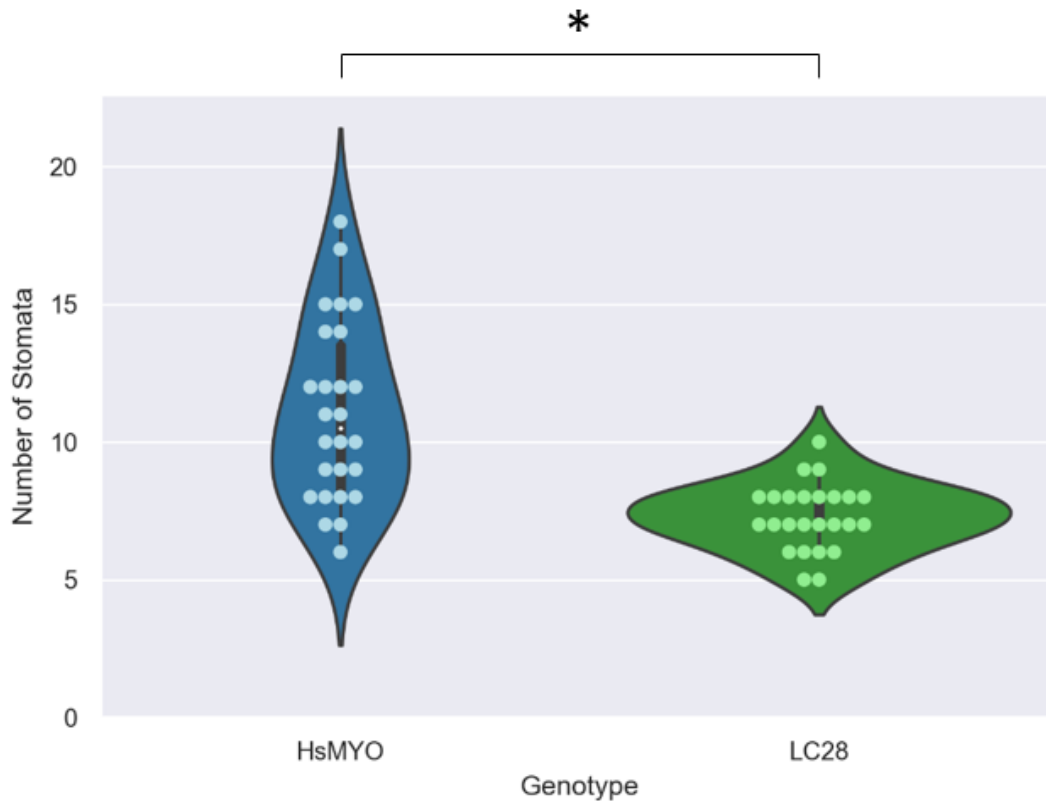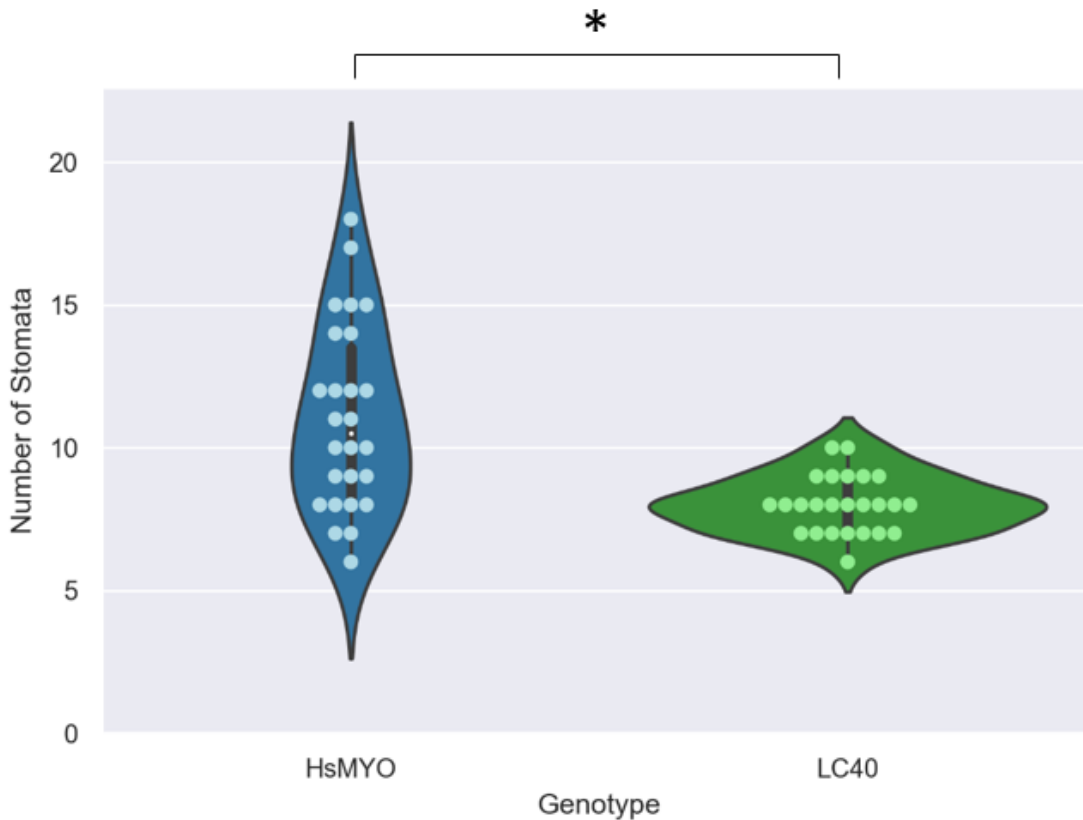**Figure 14: Double-blinded Stomatal Density Assay of LC40 and HsMYO Plants.**

Stomatal density assays comparing the average number of stomata between LC40 and HsMYO plants. A two-tailed t-test between the two groups yields a p-value < .01. The fifth true leaf of five different plants from each condition were harvested as samples. Five different images from each sample were taken via bright-field microscopy, totaling 25 images per genotype. The HsMYO data for all stomatal density assays is the same because all images were captured in the same experimental set.

A different F-box protein targeting amiRNA line is LC41 which was predicted to

downregulate other non-overlapping F-Box mRNAs compared to LC40 amiRNA targets. LC41

plants had a relatively similar stomatal conductance to the control HsMYO plants at ambient

CO_2 concentrations and responded to low CO_2 treatment albeit with a slower stomatal opening

rate when compared to HsMYO plants (Figure 15). However, when exposed to high CO_2

concentrations, LC41 plants responded much slower and ultimately remained at a much higher

stomatal conductance relative to control plants. There was no statistically significant difference

in stomatal density between LC41 and control plants, although the median was slightly lower for LC41 plants (Figure 16). Through bioinformatic database mining, one of the amiRNA targeted loci in LC41 plants was found to have a predicted primary interaction with Sugar Transport 4 (STP4), a sugar transporter recently shown to have an effect on stomatal opening and closure (Figure 17, Flütsch et al., 2020). Additionally, through bioinformatic analysis it was shown that STP4 interacts with Plasma Membrane Intrinsic Protein 2;1 (AtPIP2;1), a known aquaporin involved in CO_2 signaling (Figure 18, Bellati et al., 2016). Furthermore, through bioinformatic analysis it was shown that one of the amiRNA targeted loci in LC41 plants has a secondary interaction with known CO_2 signaling component Two Pore K Channel 1 (TPK1) through Heat Stable 1 (HS1), a protein involved in plant stress response (Figure 38, bioGRID).
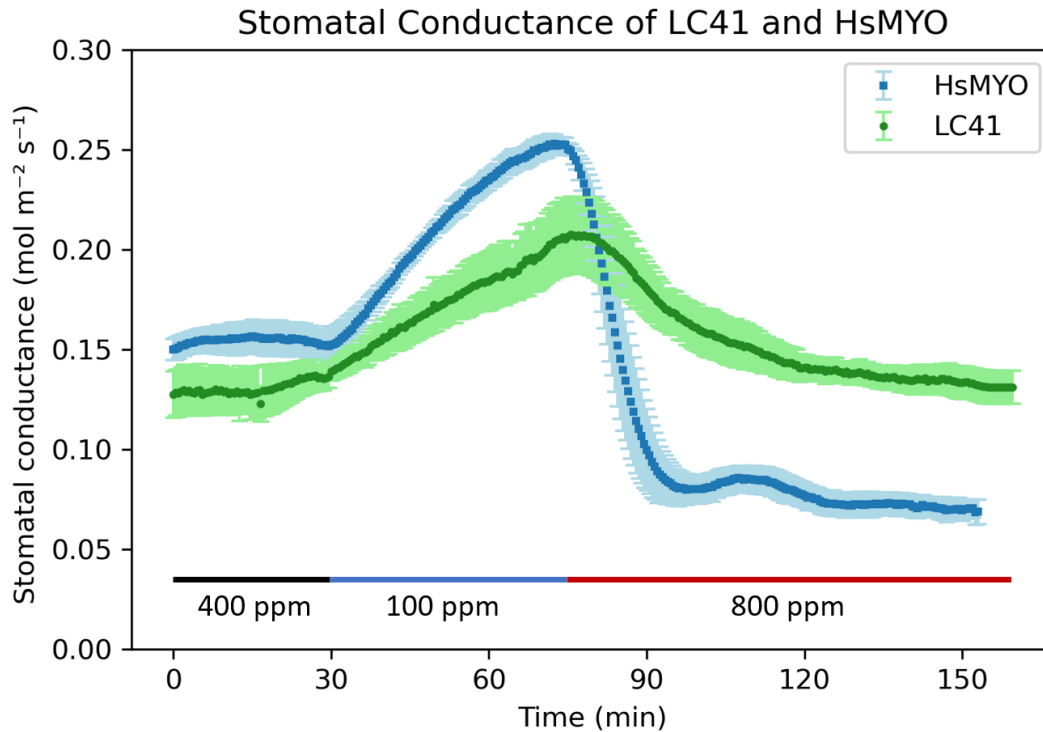
Figure 15: Stomatal Conductance of an F-box Protein Targeting amiRNA Line (LC41) and Control (HsMYO) Plants in Response to Imposed Shifts in [CO2].

Time course assay of LC41 and HsMYO plant leaves in response to [CO_2]. Stomatal conductance was measured in leaves exposed to ambient CO_2 (400 ppm) for 30 minutes, low CO_2 (100 ppm) for 45 minutes, and high CO_2 (800 ppm) for 80 minutes. Stomatal conductance is a measurement of the rate of CO_2 entering or water vapor exiting the stomata; higher stomatal conductance indicates a larger stomatal opening. Data represent the mean ± SEM of three leaves from different 5–6-week-old plants.
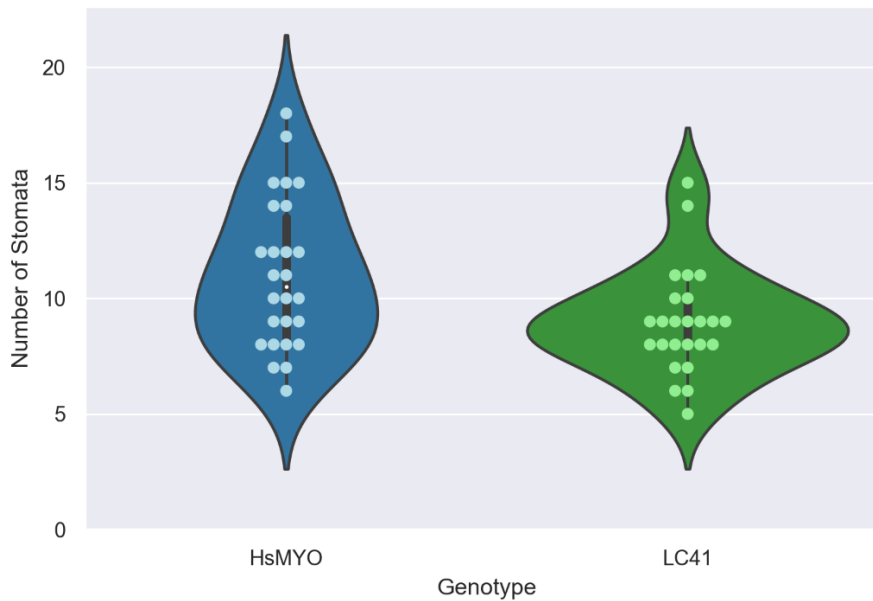
Figure 16: Double-blinded Stomatal Density Assay of LC41 and HsMYO Plants.

Stomatal density assays comparing the average number of stomata between LC41 and HsMYO plants. A two-tailed t-test between the two groups yields a p-value >.01. The fifth true leaf of five different plants from each condition were harvested as samples. Five different images from each sample were taken via bright-field microscopy, totaling 25 images per genotype. The HsMYO data for all stomatal density assays is the same because all images were captured in the same experimental set.
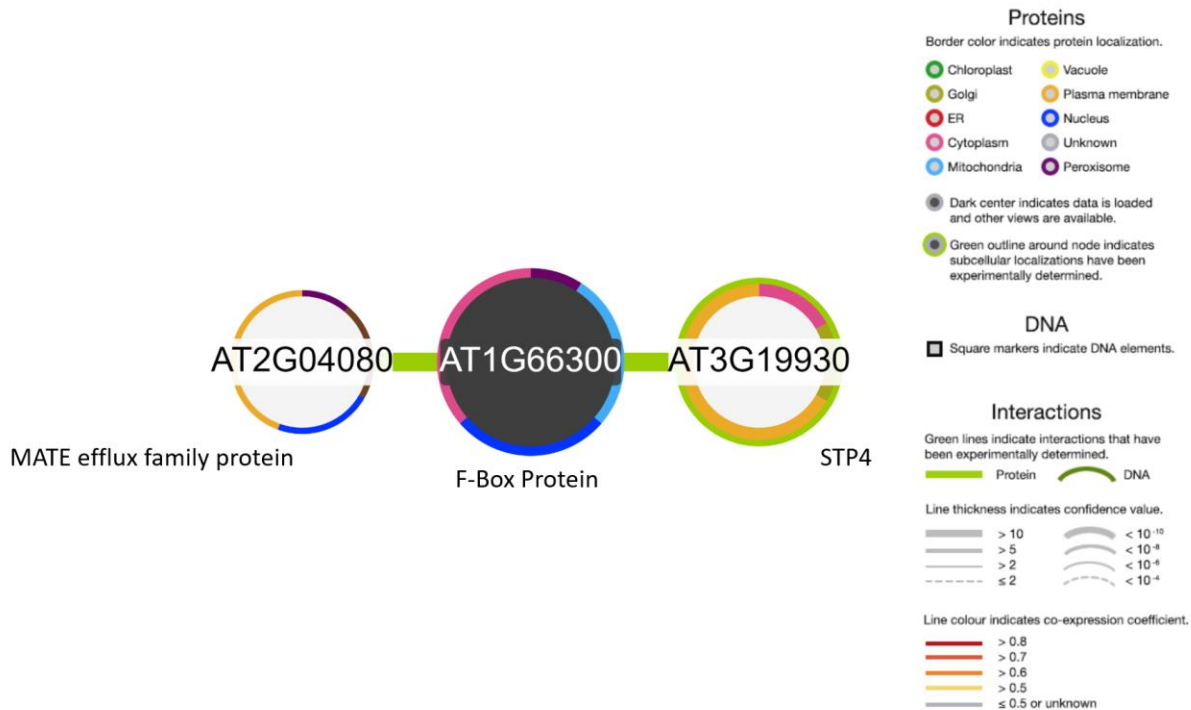
Figure 17: Interactome of amiRNA Targeted Locus AT1G66300.

Interactome of an F-box protein (locus AT1G66300) shown to interact with two proteins from published datasets: Sugar Transporter 4 (STP4) and a MATE efflux family protein as provided by the ePlant Interaction viewer (Waese et al., 2017).
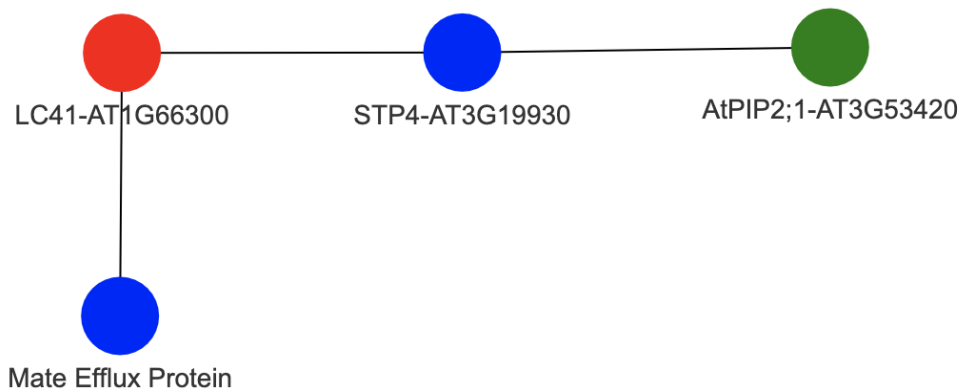
Figure 18: Interactome of amiRNA Targeted Locus AT1G66300.

Interactome of an F-box protein (locus AT1G66300) shown to interact with two proteins from published datasets: Sugar Transporter 4 (STP4) and a MATE efflux family protein. STP4 was shown to interact with AtPIP2; 1 through a published paper. Red genes signify an amiRNA loci target in candidate line, blue genes signify primary interactors with amiRNA loci target, and green genes signify known CO_2 signaling components.

LC42, a candidate plant line with a silenced 40S Ribosomal S19 Family protein, was able to respond to changes in CO_2 (Figure 19). At ambient CO_2 concentrations, LC42 plants had a much lower stomatal conductance than the control. Once treated with low CO_2, both genotypes responded and showed a much higher stomatal conductance. After high CO_2 treatment, LC42 and HsMYO plants both had much lower stomatal conductance. However, at ambient, low, and high CO_2 concentrations, the stomatal conductance of LC42 plants was much lower relative to HsMYO plants. The stomatal density data reveals there was a large statistically significant difference in the number of stomata between LC42 and control plants, accounting for the lower stomatal conductance at ambient CO_2 ($p < .0001$, Swink, K. 2021). The relatively large effect on stomatal density warrants further investigation.
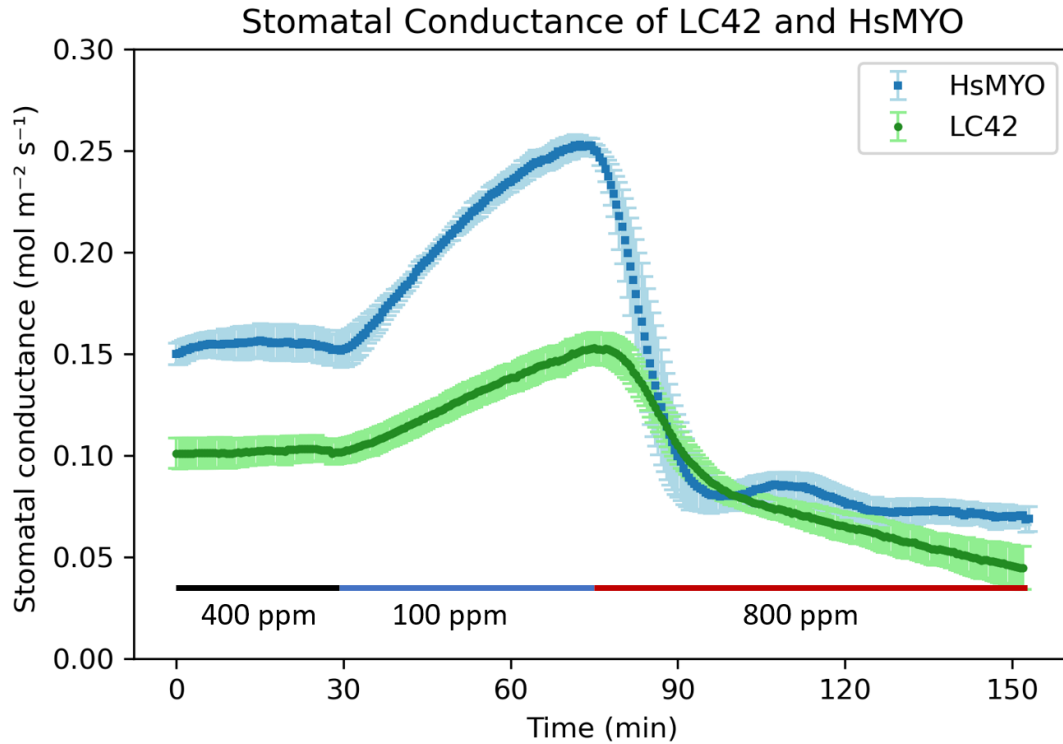
Figure 19: Stomatal Conductance of a 40S Ribosomal S19 Family Protein Targeting amiRNA Line (LC42) and Control (HsMYO) Plants in Response to Imposed Shifts in [CO2].

Time course assay of LC42 and HsMYO plant leaves in response to $[CO_2]$. Stomatal conductance was measured in leaves exposed to ambient CO_2 (400 ppm) for 30 minutes, low CO_2 (100 ppm) for 45 minutes, and high CO_2 (800 ppm) for 80 minutes. Stomatal conductance is a measurement of the rate of CO_2 entering or water vapor exiting the stomata; higher stomatal conductance indicates a larger stomatal opening. Data represent the mean ± SEM of three leaves from different 5–6-week-old plants.

LC43 plants, a 40S Ribosomal S26e family protein targeting amiRNA line, had slightly cooler leaves on average compared to the wild-type control HsMYO plants at ambient CO_2 conditions (Figure 20). LC43 plants responded to changes in CO_2 (Figure 21). At ambient CO_2 concentrations, LC43 plants had a slightly lower stomatal conductance but responded in the same manner as the control plants to low CO_2. When exposed to high CO_2 concentrations, LC43 plants responded initially the same as control plants but did not decrease as much in stomatal conductance after 120 minutes of high CO_2 treatment. Interestingly, the stomatal density data reveals there was a large statistically significant difference in the number of stomata between LC43 and control plants, but this only had a marginal effect on the stomatal conductance at ambient CO_2 concentrations ($p < .0001$, Swink, K. 2021). Further repeat experiments would be needed to assess the robustness of this stomatal development phenotype.

Figure 20: Bright-Field and Infrared Temperature Images of a 40S Ribosomal S26e Family Protein Targeting amiRNA Line (LC43) and Control (HsMYO) Plants at Ambient [CO2].

Images of candidate and control plants highlighting the temperature of the plant leaves at ambient [CO_2] - 415 ppm. Images are representative samples from 3–4-week plants of each plant line.

Figure 21: Stomatal Conductance of LC43 and HsMYO Plants in Response to Imposed Shifts in [CO2].

Time course assay of LC43 and HsMYO plant leaves in response to [CO_2]. Stomatal conductance was measured in leaves exposed to ambient CO_2 (400 ppm) for 30 minutes, low CO_2 (100 ppm) for 45 minutes, and high CO_2 (800 ppm) for 80 minutes. Stomatal conductance is a measurement of the rate of CO_2 entering or water vapor exiting the stomata; higher stomatal conductance indicates a larger stomatal opening. Data represent the mean ± SEM of three leaves from different 5–6-week-old plants.

LC48 plants had a downregulated Sec14p-like Phosphatidylinositol transfer family protein and had much cooler leaves on average compared to the control HsMYO plants at ambient CO_2 conditions (Figure 22). LC48 plants and HsMYO plants responded to changes in CO_2 (Figure 23). Both LC48 and control plants showed a highly increased stomatal conductance in response to low CO_2 treatment, with LC48 plants increasing marginally less. Additionally, both plants showed a decreased stomatal conductance in response to high CO_2 treatment. The stomatal densities between the LC48 and HsMYO plants were very similar, resulting in no statistically significant difference in the number of stomata between the two genotypes (Figure 24).
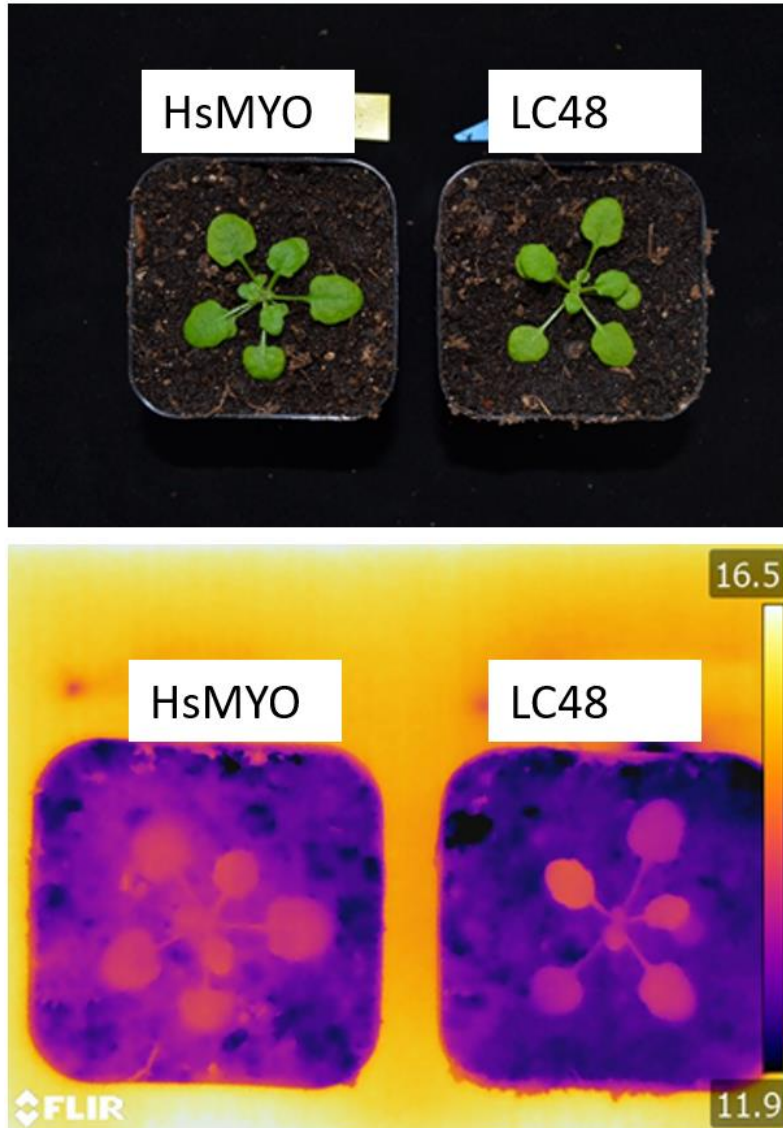
Figure 22: Bright-Field and Infrared Temperature Images of a Sec14p-like Phosphatidylinositol Transfer Family Protein Targeting amiRNA Line (LC48) and Control (HsMYO) Plants at Ambient [CO2].

Images of candidate and control plants highlighting the temperature of the plant leaves at ambient [CO_2] - 415 ppm. Images are representative samples from 3–4-week plants of each plant line.
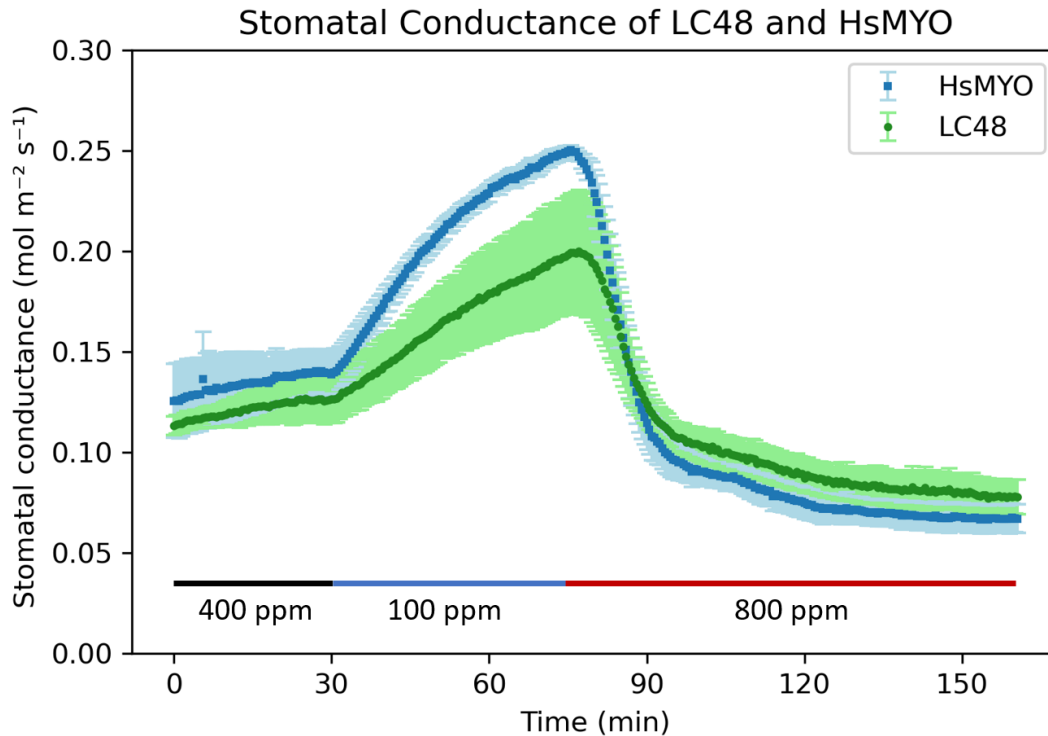
Figure 23: Stomatal Conductance of LC48 and HsMYO Plants in Response to Imposed Shifts in [CO2].

Time course assay of LC48 and HsMYO plant leaves in response to [CO_2]. Stomatal conductance was measured in leaves exposed to ambient CO_2 (400 ppm) for 30 minutes, low CO_2 (100 ppm) for 45 minutes, and high CO_2 (800 ppm) for 80 minutes. Stomatal conductance is a measurement of the rate of CO_2 entering or water vapor exiting the stomata; higher stomatal conductance indicates a larger stomatal opening. Data represent the mean ± SEM of three leaves from different 5–6-week-old plants.
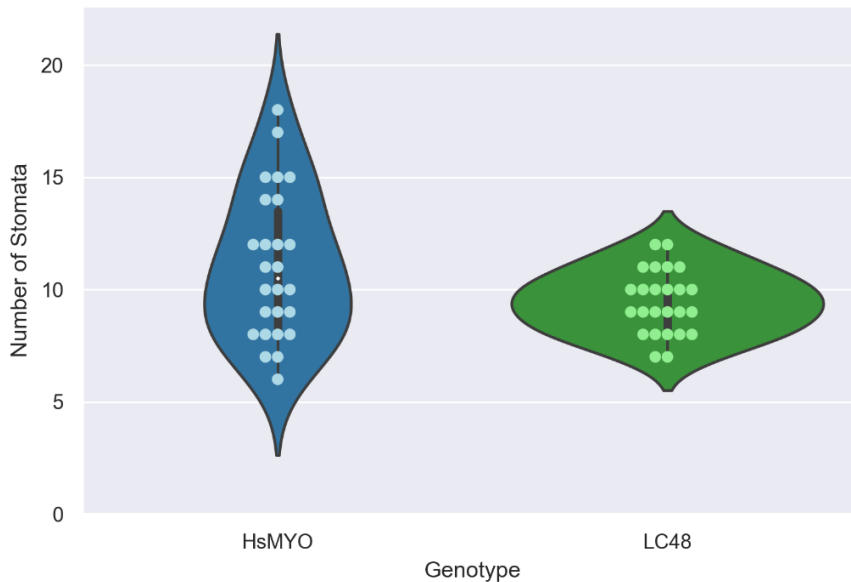
Figure 24: Double-blinded Stomatal Density Assay of LC48 and HsMYO Plants.

Stomatal density assays comparing the average number of stomata between LC48 and HsMYO plants. A two-tailed t-test between the two groups yields a p-value > .01. The fifth true leaf of five different plants from each condition were harvested as samples. Five different images from each sample were taken via bright-field microscopy, totaling 25 images per genotype. The HsMYO data for all stomatal density assays is the same because all images were captured in the same experimental set.

LC51 had a silenced tRNAse Z4 protein and had slightly cooler leaves on average compared to the control HsMYO plants at ambient CO_2 conditions (Figure 25). LC51 plants and HsMYO plants responded to changes in CO_2 (Figure 26). Both LC51 and control plants showed a highly increased stomatal conductance in response to low CO_2 treatment. Additionally, both plants showed a decreased stomatal conductance in response to high CO_2 treatment. The stomatal densities between the LC51 and HsMYO plants were very similar, resulting in no statistically significant difference in the number of stomata between the two genotypes (Figure 27).
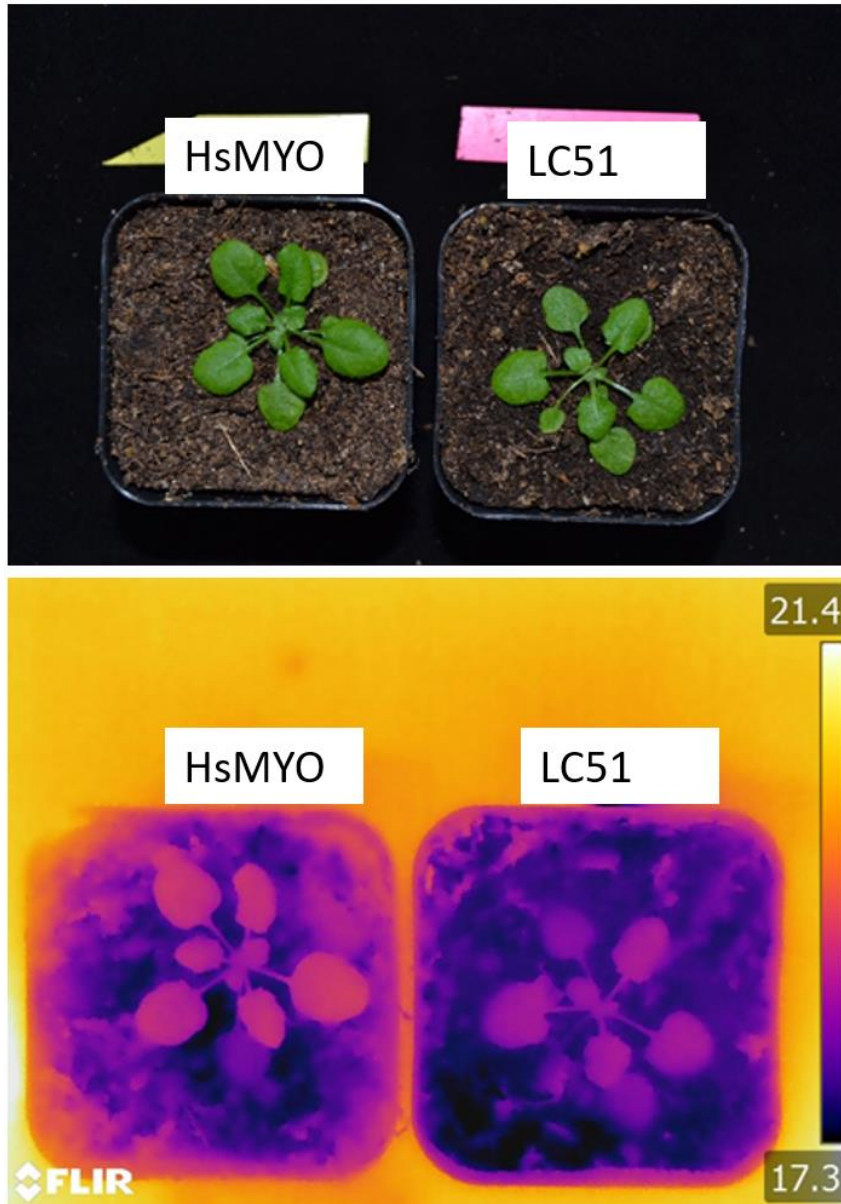
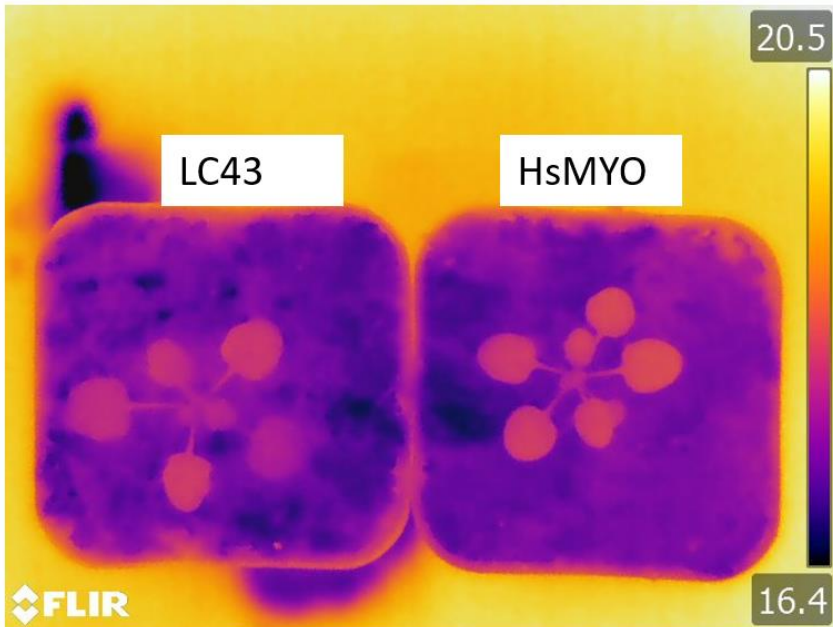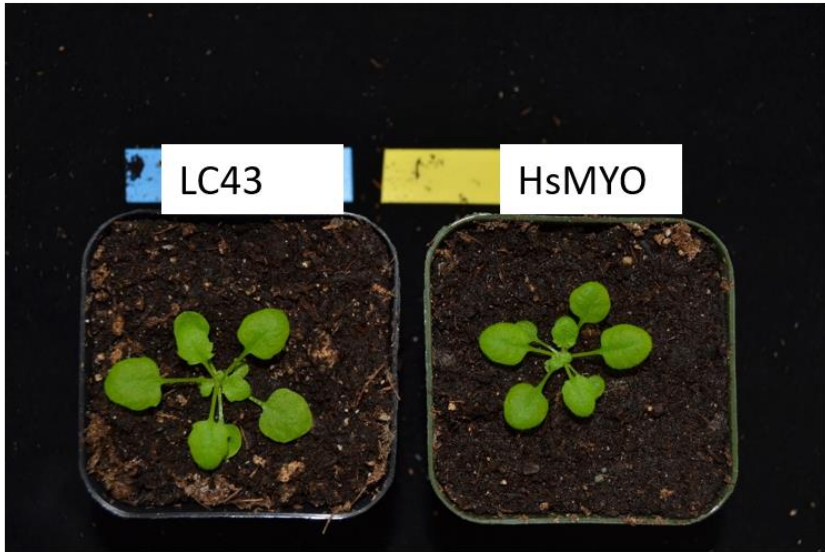**Figure 25: Bright-Field and Infrared Temperature Images of a tRNAse Z4 Protein Targeting amiRNA Line (LC51) and Control (HsMYO) Plants at Ambient [CO2].**

Images of candidate and control plants highlighting the temperature of the plant leaves at ambient $[CO_2]$ - 415 ppm. Images are representative samples from 3–4-week plants of each plant line.
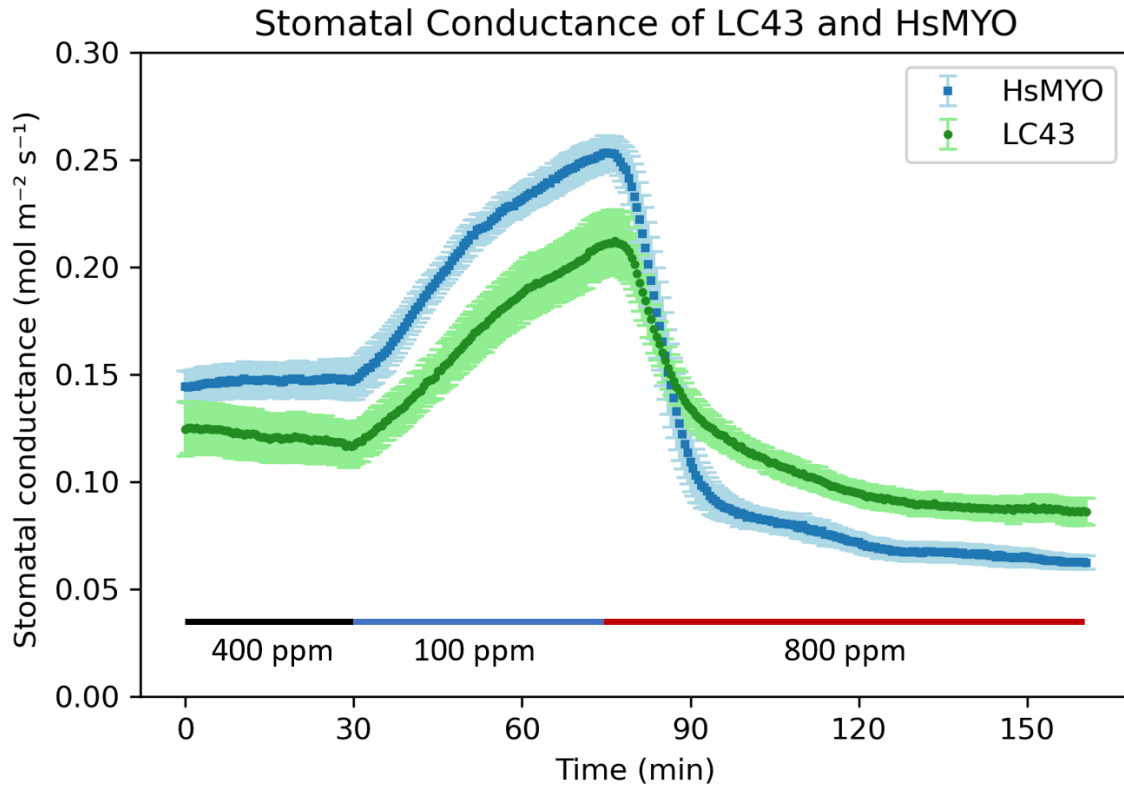
Figure 26: Stomatal Conductance of LC51 and HsMYO Plants in Response to Imposed Shifts in [CO2].

Time course assay of LC51 and HsMYO plant leaves in response to [CO_2]. Stomatal conductance was measured in leaves exposed to ambient CO_2 (400 ppm) for 30 minutes, low CO_2 (100 ppm) for 45 minutes, and high CO_2 (800 ppm) for 80 minutes. Stomatal conductance is a measurement of the rate of CO_2 entering or water vapor exiting the stomata; higher stomatal conductance indicates a larger stomatal opening. Data represent the mean ± SEM of three leaves from different 5–6-week-old plants.

Figure 27: Double-blinded Stomatal Density Assay of LC51 and HsMYO Plants.

Stomatal density assays comparing the average number of stomata between LC51 and HsMYO plants. A two-tailed t-test between the two groups yields a p-value > .01. The fifth true leaf of five different plants from each condition were harvested as samples. Five different images from each sample were taken via bright-field microscopy, totaling 25 images per genotype. The HsMYO data for all stomatal density assays is the same because all images were captured in the same experimental set.

LC35, a plant line with an amiRNA predicted to downregulate transcription factor jumonji proteins, had a heavily affected response in stomatal conductance to changes in CO_2-mediated stomatal conductance compared to control plants (Figure 28). LC35 plants had a higher stomatal conductance at ambient CO2 conditions relative to HsMYO plants but were severely impaired in responding to low CO_2 treatment compared to HsMYO plants. Further, LC35 plants responded extremely slowly to high CO_2 treatment compared to HsMYO plants and remained at a relatively high stomatal conductance even after 120 minutes. The stomatal density reveals a significance difference in the number of stomata between LC35 and HsMYO plants ($p < .01$, Swink, K. 2021).
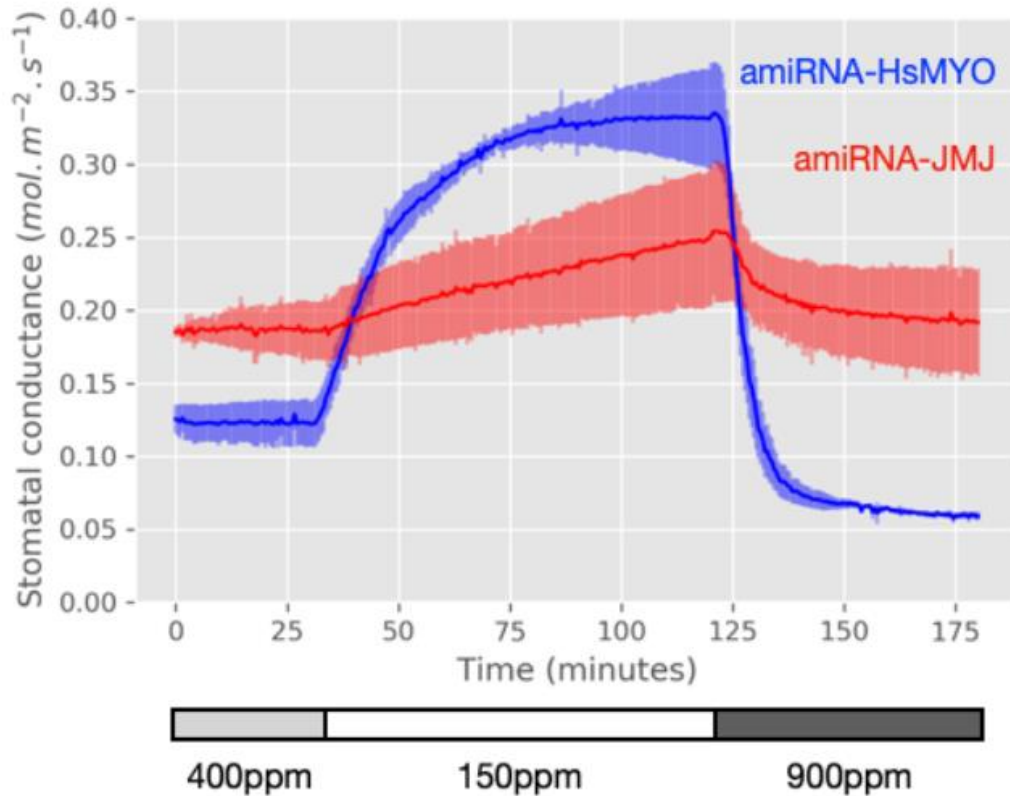
Figure 28: Stomatal Conductance of a Transcription Factor Jumonji Family Protein Targeting amiRNA Line (LC35) and Control (HsMYO) Plants in Response to Imposed Shifts in [CO2].

Time course assay of LC35 and HsMYO plant leaves in response to [CO_2]. Stomatal conductance was measured in leaves exposed to ambient CO_2 (400 ppm) for 30 minutes, low CO_2 (100 ppm) for 45 minutes, and high CO_2 (800 ppm) for 80 minutes. Stomatal conductance is a measurement of the rate of CO_2 entering or water vapor exiting the stomata; higher stomatal conductance indicates a larger stomatal opening. Data represent the mean ± SEM of three leaves from different 5–6-week-old plants.

Another transcription factor jumonji protein targeting amiRNA line was LC56, which interestingly targeted two of the same loci as LC35. LC56 plants had much cooler leaves on average compared to the wild-type control HsMYO plants at ambient CO_2 conditions (Figure 29). However, this mutant was not affected in terms of CO_2-mediated stomatal conductance at ambient, low, or high CO_2 concentrations. Both LC56 and control plants showed a highly increased stomatal conductance in response to low CO_2 treatment (Figure 30). Additionally, both

plants showed a decreased stomatal conductance in response to high CO_2 treatment. The stomatal

density reveals a significance difference in the number of stomata between LC56 and HsMYO

plants ($p < .01$, Figure 31).
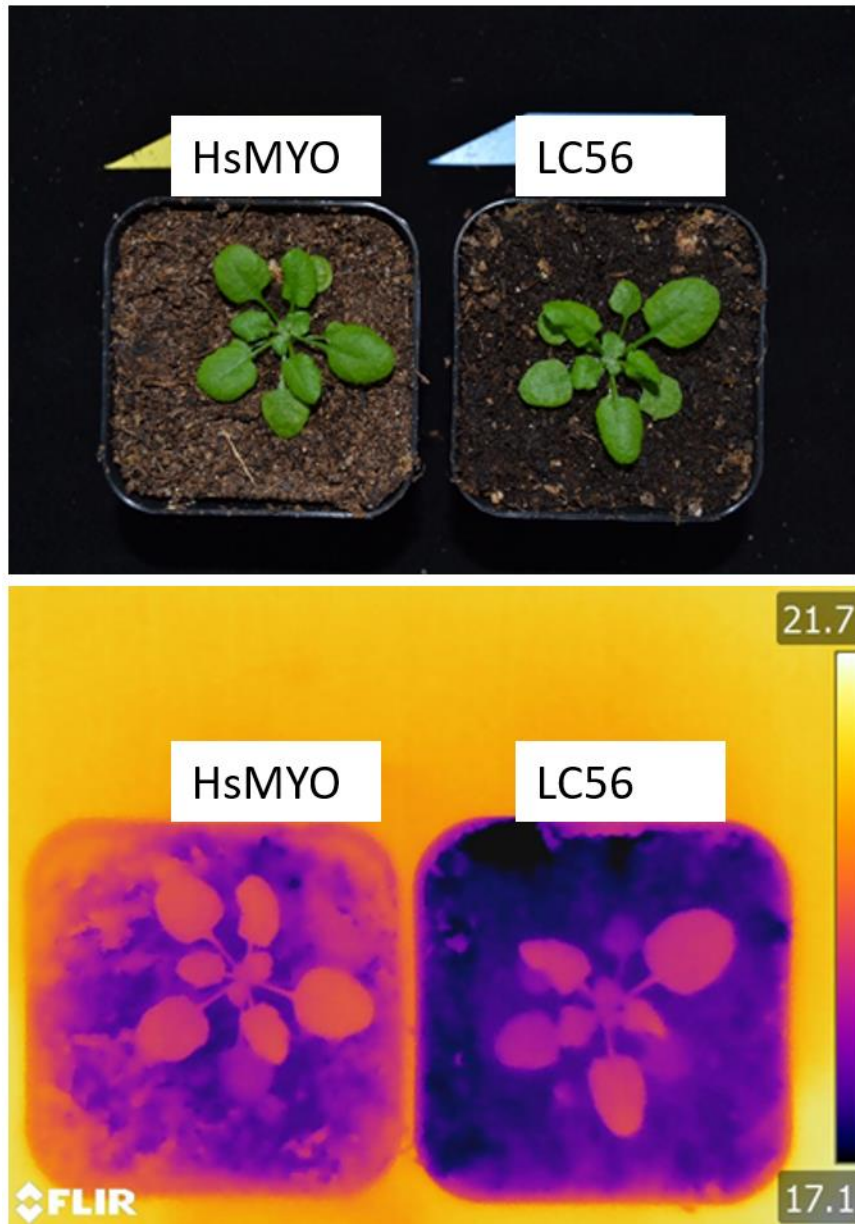
Figure 29: Bright-Field and Infrared Temperature Images of a Transcription Factor Jumonji Family Protein Targeting amiRNA Line (LC56) and Control (HsMYO) Plants at Ambient [CO2].

Images of candidate and control plants highlighting the temperature of the plant leaves at ambient [CO_2] - 415 ppm. Images are representative samples from 3–4-week plants of each plant line.
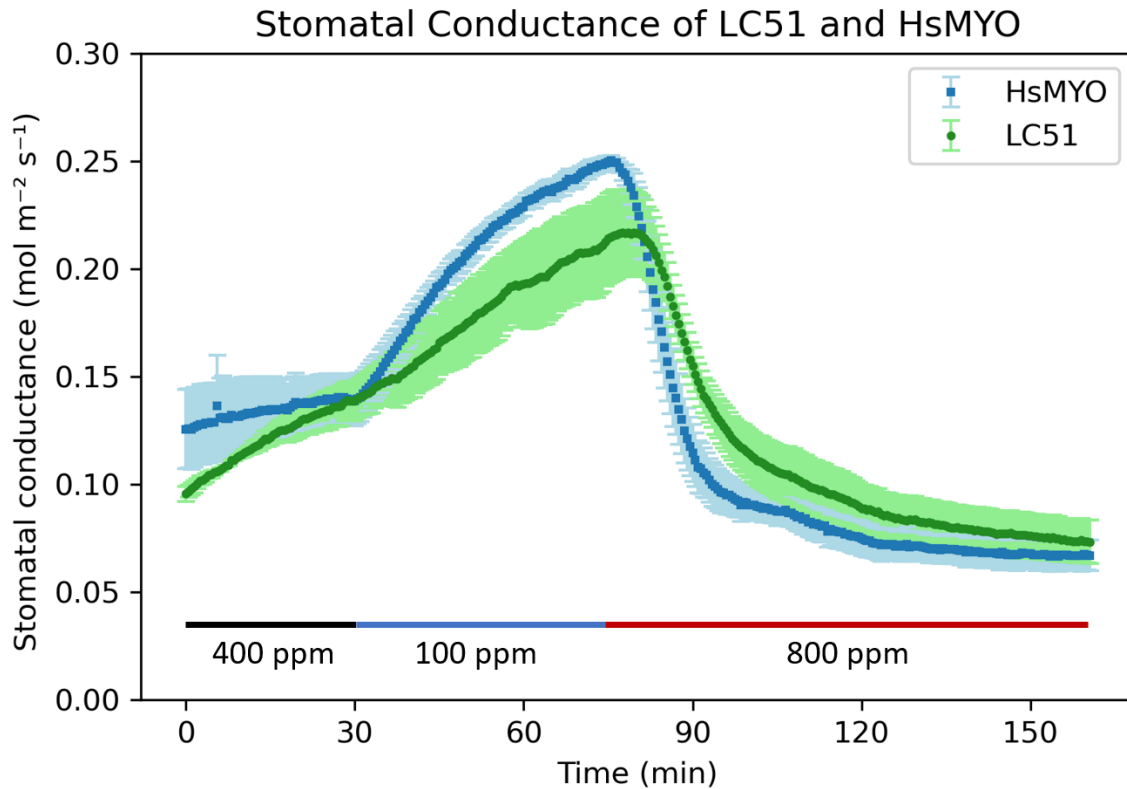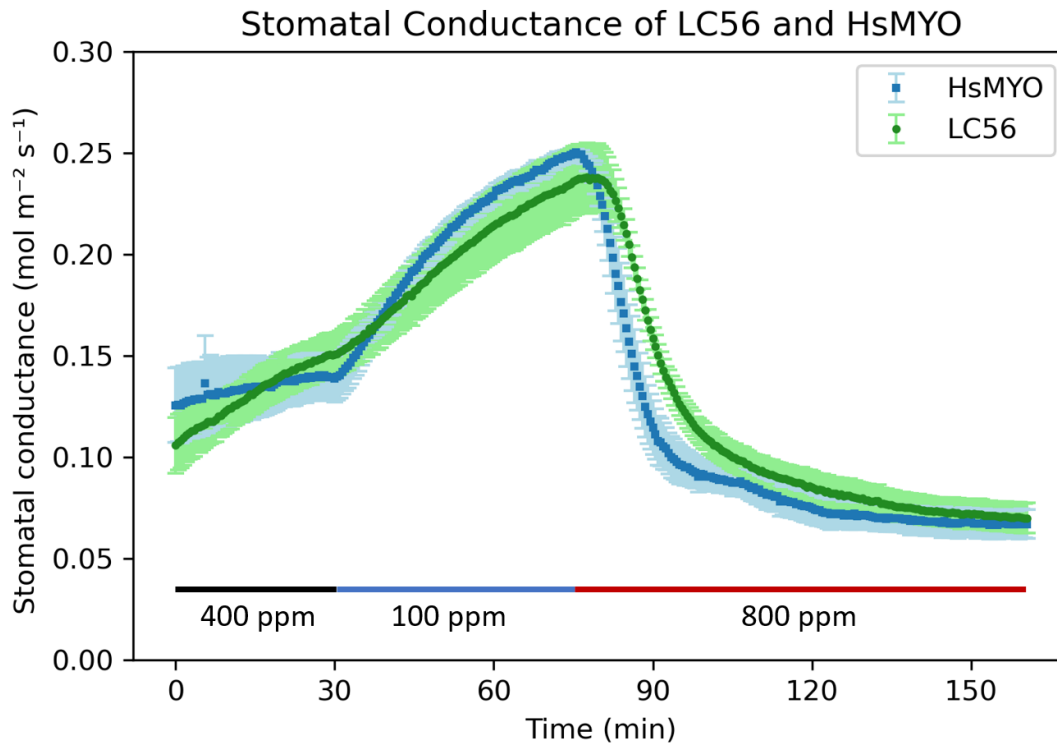
Figure 30: Stomatal Conductance of LC56 and HsMYO Plants in Response to Imposed Shifts in [CO2].

Time course assay of LC56 and HsMYO plant leaves in response to [CO_2]. Stomatal conductance was measured in leaves exposed to ambient CO_2 (400 ppm) for 30 minutes, low CO_2 (100 ppm) for 45 minutes, and high CO_2 (800 ppm) for 80 minutes. Stomatal conductance is a measurement of the rate of CO_2 entering or water vapor exiting the stomata; higher stomatal conductance indicates a larger stomatal opening. Data represent the mean ± SEM of three leaves from different 5–6-week-old plants.
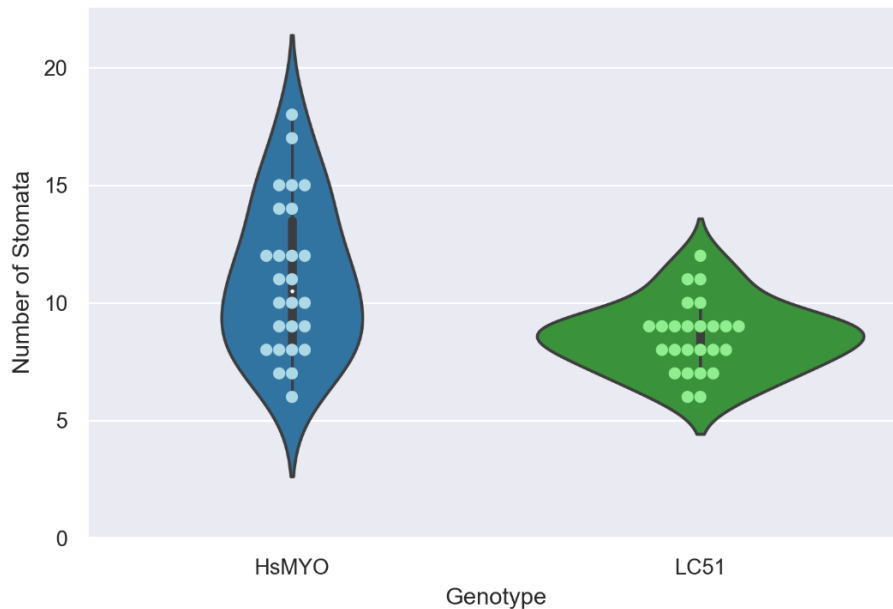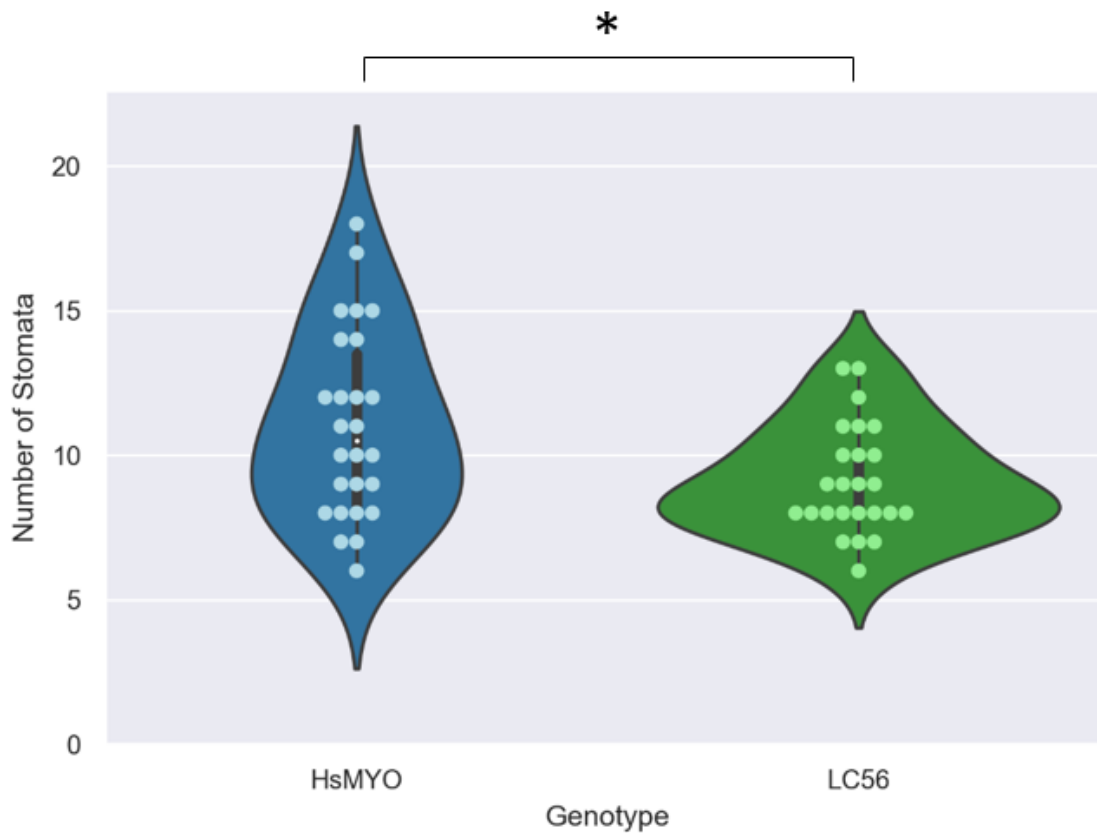
Figure 31: Double-blinded Stomatal Density Assay of LC56 and HsMYO Plants.

Stomatal density assays comparing the average number of stomata between LC56 and HsMYO plants. A two-tailed t-test between the two groups yields a p-value < .01. The fifth true leaf of five different plants from each condition were harvested as samples. Five different images from each sample were taken via bright-field microscopy, totaling 25 images per genotype. The HsMYO data for all stomatal density assays is the same because all images were captured in the same experimental set.

LC57, a TRAF-like family protein targeting amiRNA line, had much cooler leaves on average compared to the wild-type control HsMYO plants at ambient CO_2 conditions (Figure 32). LC57 plants and HsMYO control plants responded to changes in CO_2 (Figure 33). Both LC57 and control plants showed a highly increased stomatal conductance in response to low CO_2 treatment. Additionally, both plants showed a decreased stomatal conductance in response to high CO_2 treatment.
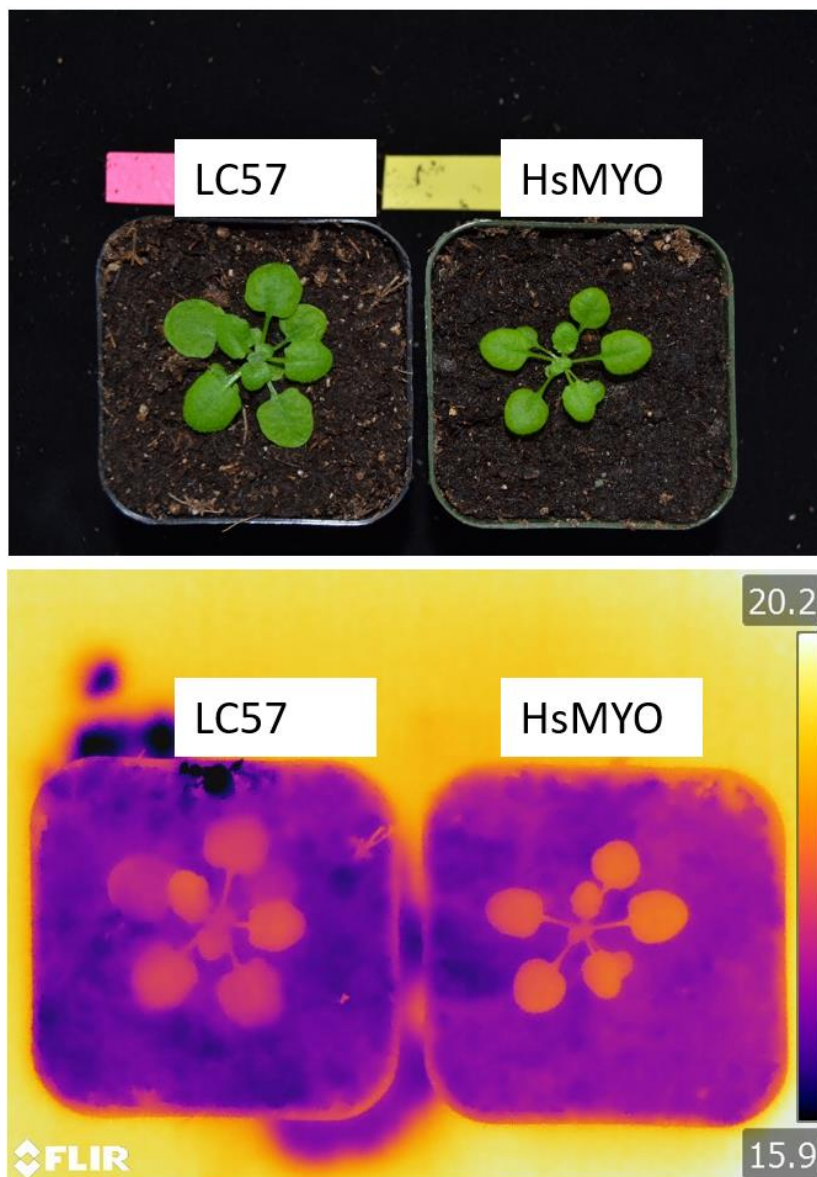
Figure 32: Bright-Field and Infrared Temperature Images of a TRAF-like Family Protein Targeting amiRNA Line (LC57) and Control (HsMYO) Plants at Ambient [CO2].

Images of candidate and control plants highlighting the temperature of the plant leaves at ambient [CO_2] - 415 ppm. Images are representative samples from 3–4-week plants of each plant line.
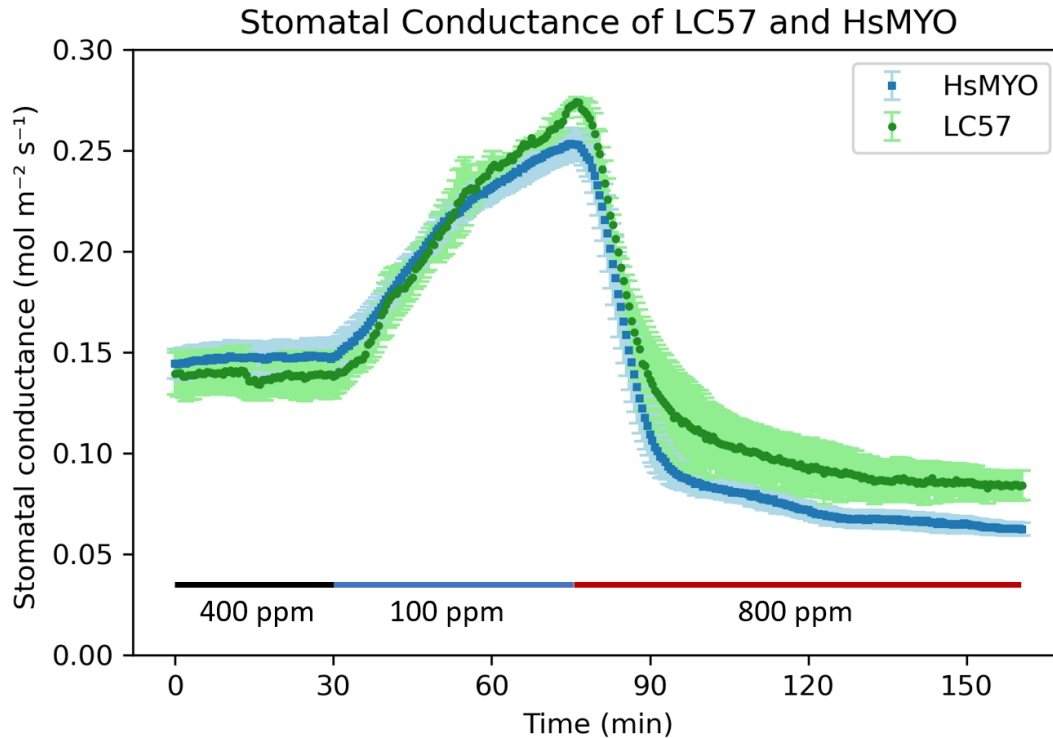
Figure 33: Stomatal Conductance of LC57 and HsMYO Plants in Response to Imposed Shifts in [CO2].

Time course assay of LC57 and HsMYO plant leaves in response to [CO_2]. Stomatal conductance was measured in leaves exposed to ambient CO_2 (400 ppm) for 30 minutes, low CO_2 (100 ppm) for 45 minutes, and high CO_2 (800 ppm) for 80 minutes. Stomatal conductance is a measurement of the rate of CO_2 entering or water vapor exiting the stomata; higher stomatal conductance indicates a larger stomatal opening. Data represent the mean ± SEM of three leaves from different 5–6-week-old plants.

LC71 plants were predicted to down regulate phototropic-responsive NPH3 family proteins and had a heavily affected response in stomatal conductance to changes in CO_2-mediated stomatal conductance compared to control plants (Figure 34). Both LC71 and HsMYO plants had a similar stomatal conductance at ambient CO_2 concentrations, but when exposed to low CO_2 concentrations, LC71 plants had a much slower response compared to HsMYO plants. Additionally, LC71 plants responded slowly to high CO_2 treatment and did not reach the same level of stomatal conductance as the control, even after 120 minutes of high CO_2 exposure. Interestingly, the locus AT1G30440 targeted in LC71 plants is predicted to interact with known

CO₂ signaling components Beta Carbonic Anhydrase 1 and 4 (BCA1, BCA4), TPK1, and BIG (Figure 36, Figure 37, and Figure 38). A caveat to all of these potential interactions is that the intermediate interactor between the amiRNA-targeted loci and the known CO_2 signaling component is Polyubiquitin 3 (UBQ3, Figure 35). In plants, ubiquitin is conventionally used to mark proteins for degradation, but it is possible it is involved in the CO_2 signaling pathway through unconventional ubiquitination. Further analysis will be needed to ascertain the relationship of the NPH3 family proteins and their involvement in CO_2 signaling and possibly UBQ3.
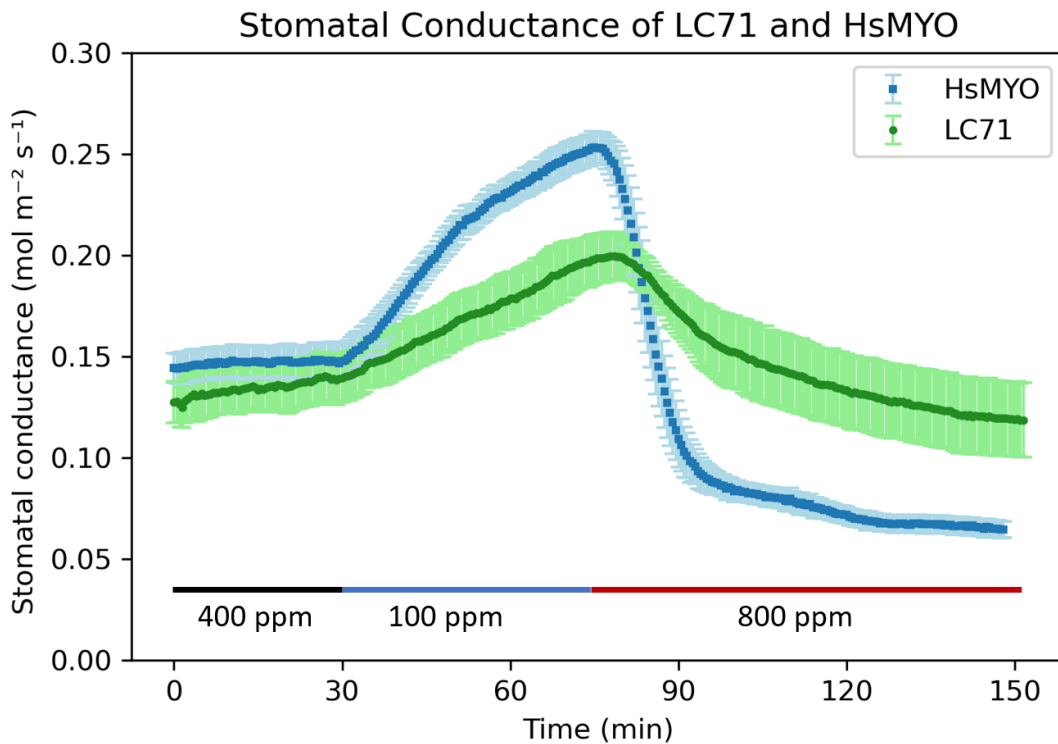
Figure 34: Stomatal Conductance of a Phototropic-responsive NPH3 Family Protein Targeting amiRNA Line (LC71) and Control (HsMYO) Plants in Response to Imposed Shifts in [CO2].

Time course assay of LC71 and HsMYO plant leaves in response to [CO₂]. Stomatal conductance was measured in leaves exposed to ambient CO_2 (400 ppm) for 30 minutes, low CO_2 (100 ppm) for 45 minutes, and high CO_2 (800 ppm) for 80 minutes. Stomatal conductance is a measurement of the rate of CO_2 entering or water vapor exiting the stomata; higher stomatal conductance indicates a larger stomatal opening. Data represent the mean ± SEM of three leaves from different 5–6-week-old plants.
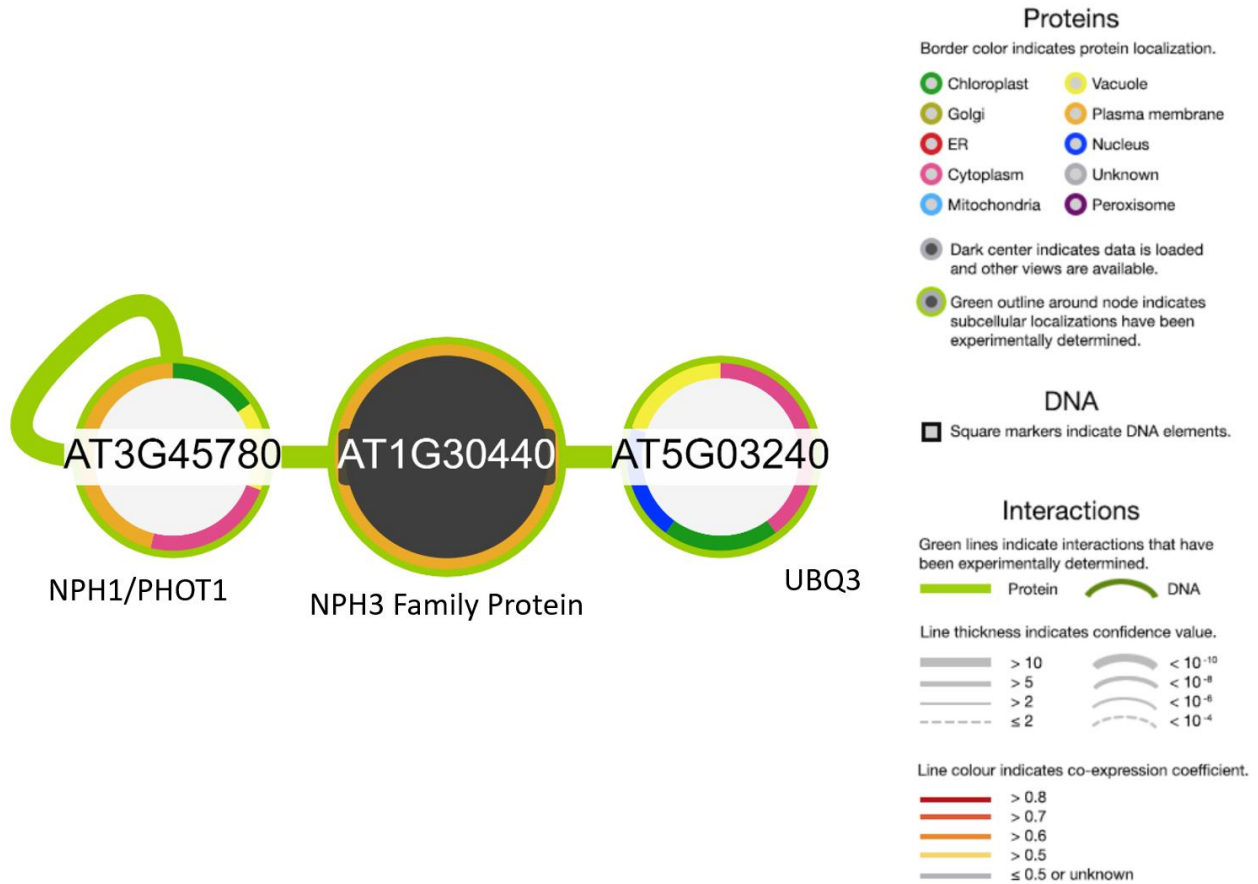
Figure 35: Interactome of amiRNA Targeted Locus AT1G30440.

Interactome of an NPH3 family protein (locus AT1G30440) shown to interact with two proteins from published datasets: Phototropin 1 (NPH1 or PHOT1) and Polyubiquitin 3 (UBQ3) as provided by the ePlant Interaction viewer (Waese et al., 2017).
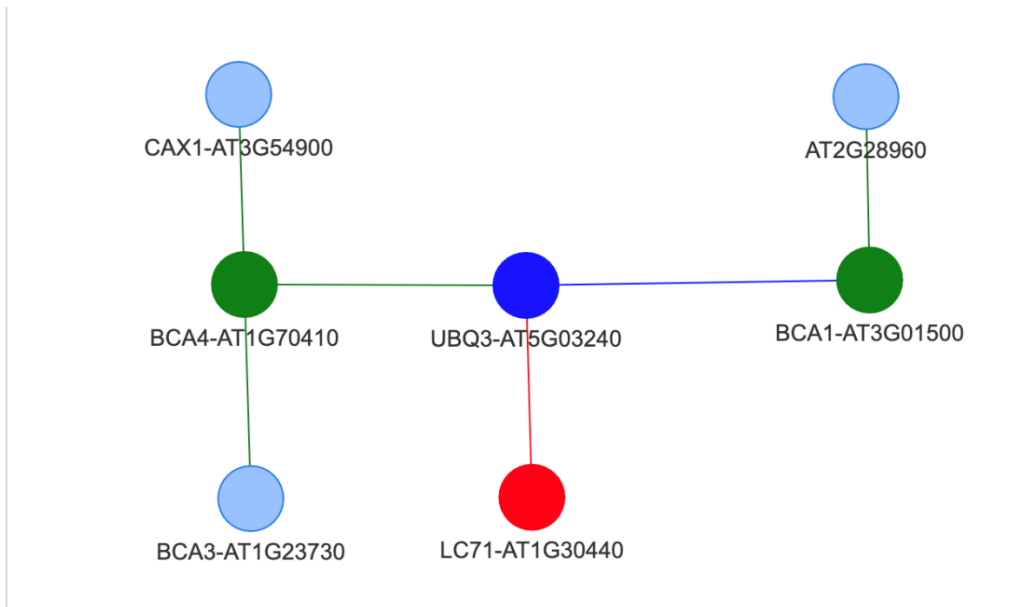
Figure 36: Interactome of amiRNA Targeted Locus AT1G30440.

Interactome of an NPH3 family protein (locus AT1G30440) shown to interact with one protein from published datasets: Polyubiquitin (UBQ3). UBQ3 was shown to interact with known CO_2 signaling components Beta Carbonic Anhydrase 1 and 4 (BCA1, BCA4) through BioGRID. Red genes signify an amiRNA loci target in candidate line, blue genes signify primary interactors with amiRNA loci target, and green genes signify known CO_2 signaling components.
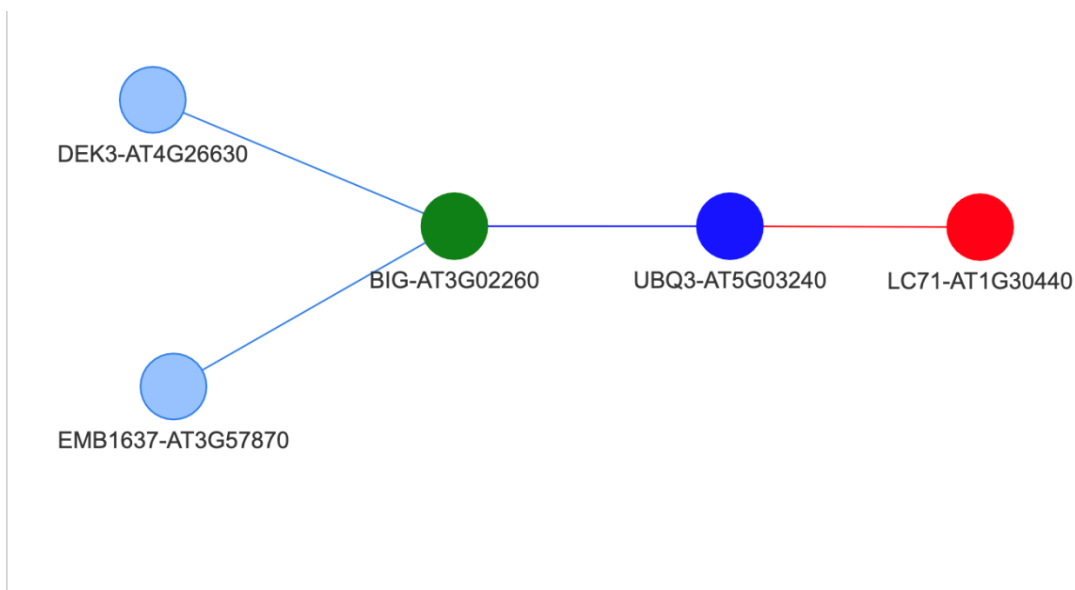
Figure 37: Interactome of amiRNA Targeted Locus AT1G30440.

Interactome of an NPH3 family protein (locus AT1G30440) shown to interact with one protein from published datasets: Polyubiquitin (UBQ3). UBQ3 was shown to interact with to interact with known CO_2 signaling component BIG through BioGRID. Red genes signify an amiRNA loci target in candidate line, blue genes signify primary interactors with amiRNA loci target, and green genes signify known CO_2 signaling components.
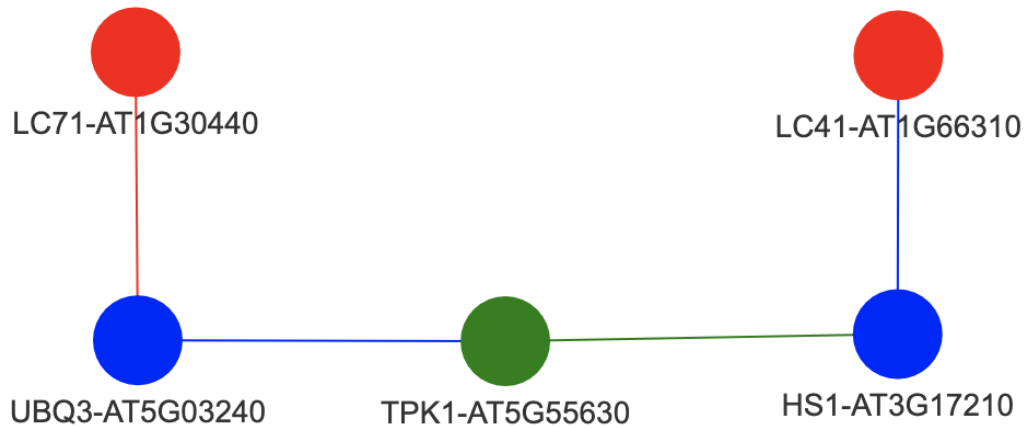
Figure 38: Interactome of amiRNA Targeted Locus AT1G66310 and AT1G30440.

Interactome of an F-box protein (locus AT1G66310) and NPH3 family protein (locus AT1G30440) shown to interact with two proteins from published datasets: Polyubiquitin (UBQ3) and Heat Stable 1 (HS1). Both UBQ3 and HS1 were shown to interact with known CO_2 signaling component Two Pore K Channel 1 (TPK1) through BioGRID. Red genes signify an amiRNA loci target in candidate line, blue genes signify primary interactors with amiRNA loci target, and green genes signify known CO_2 signaling components.

LC72 plants had an amiRNA predicted to silence tetratricopeptide repeat (TPR)-like superfamily protein homologs and had a heavily affected response in stomatal conductance to changes in CO_2-mediated stomatal conductance compared to control plants (Figure 39). Both LC72 and HsMYO plants had a similar stomatal conductance at ambient CO_2 concentrations, but when exposed to low CO_2 concentrations, LC72 plants had a much slower response compared to HsMYO plants. Additionally, LC72 plants responded slowly to high CO_2 treatment and did not reach the same level of stomatal conductance as the control, even after 120 minutes of high CO_2 exposure.
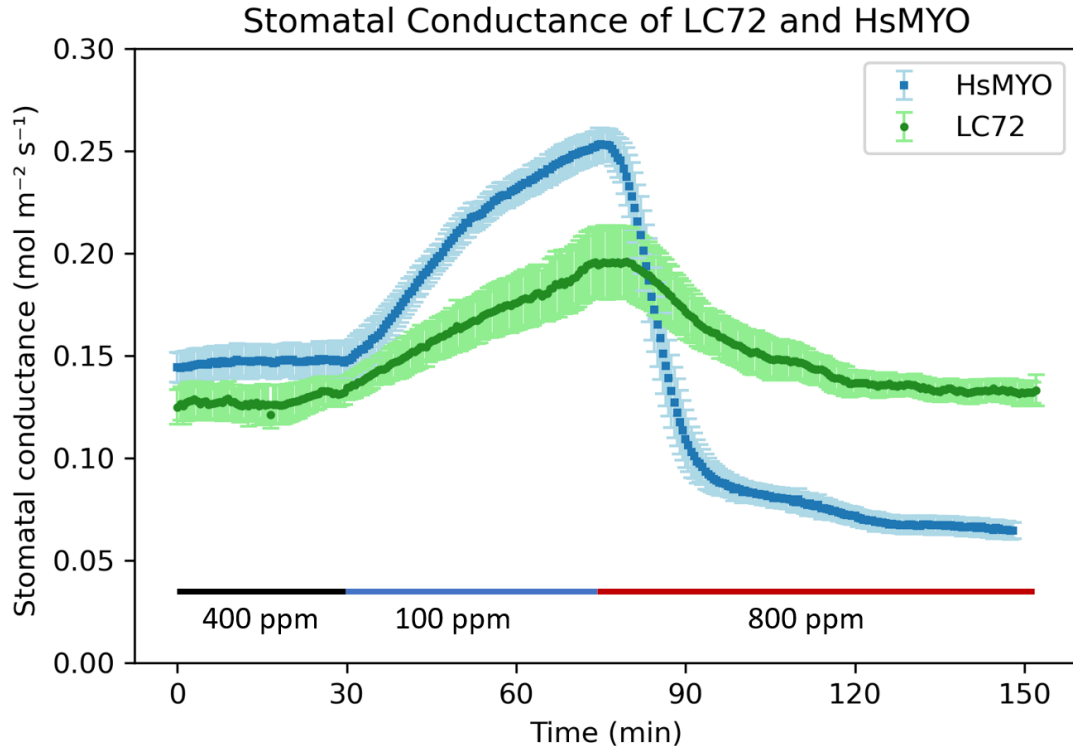
Figure 39: Stomatal Conductance of a Tetratricopeptide repeat (TPR)-like Superfamily Protein Targeting amiRNA Line (LC72) and Control (HsMYO) Plants in Response to Imposed Shifts in [CO2].

Time course assay of LC72 and HsMYO plant leaves in response to [CO_2]. Stomatal conductance was measured in leaves exposed to ambient CO_2 (400 ppm) for 30 minutes, low CO_2 (100 ppm) for 45 minutes, and high CO_2 (800 ppm) for 80 minutes. Stomatal conductance is a measurement of the rate of CO_2 entering or water vapor exiting the stomata; higher stomatal conductance indicates a larger stomatal opening. Data represent the mean ± SEM of three leaves from different 5–6-week-old plants.

Figure 40 shows the average temperature of leaves at ambient CO_2 conditions (415 ppm).

Plants were grown to 2-3 weeks and the temperature of the true leaves were taken for each

candidate and later analyzed for averages and standard deviations. Importantly, past infrared

images for the initial screen and reconfirmation screen were taken after low CO_2 treatment (150

ppm) for two hours while the current images were taken at ambient CO_2 levels. Consequently,

the temperature differences between the control line and candidate amiRNA lines are not nearly

as pronounced in these results but still provide useful information regarding leaf temperature and

stomatal conductance at ambient CO_2 conditions. Nearly all the amiRNA candidate plants had around the same average leaf temperature as the HsMYO control. Interestingly, the one outlier was LC48 with an average leaf temperature far cooler than the control.
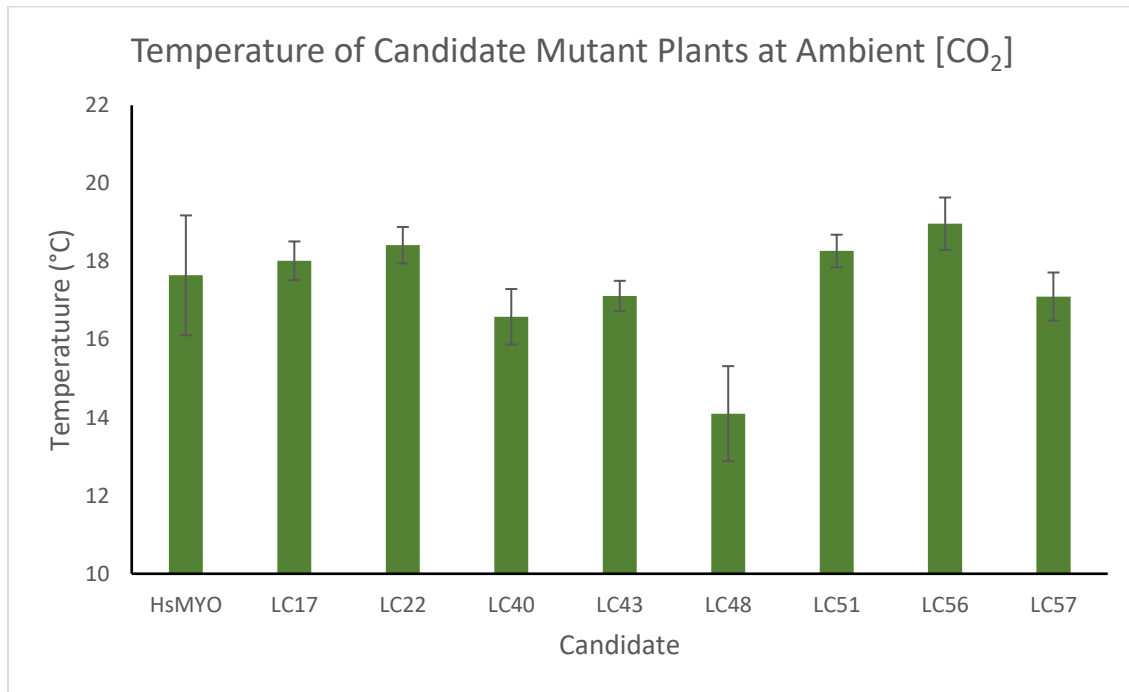
Figure 40: Average Temperature Measurements from Representative Infrared Images of Each Candidate and HsMYO at Ambient [CO2].

Average temperature measurements from infrared images at ambient [CO2]. The temperature reading is an average of the five largest leaves of each plant. The images were not captured at the same time, so no ANOVA analysis was completed. Image temperatures were analyzed via FLIR software.

Figure 41 shows an ANOVA analysis of the stomatal density for the control line and many amiRNA candidate lines. All of these plants were grown at the same time and thus leaf harvesting and microscopy were completed within the same timeframe. The control line has a similar stomatal density to most of the amiRNA lines with a few exceptions. Candidate lines LC17, LC28, and LC30 have fewer stomata compared to the control, but a Tukey-Kramer post hoc test reveals only LC30 has a statistically significant difference compared to the control in

terms of stomatal density. LC17 and LC28 do not have a statistically significant difference

compared to the control in terms of stomatal density.
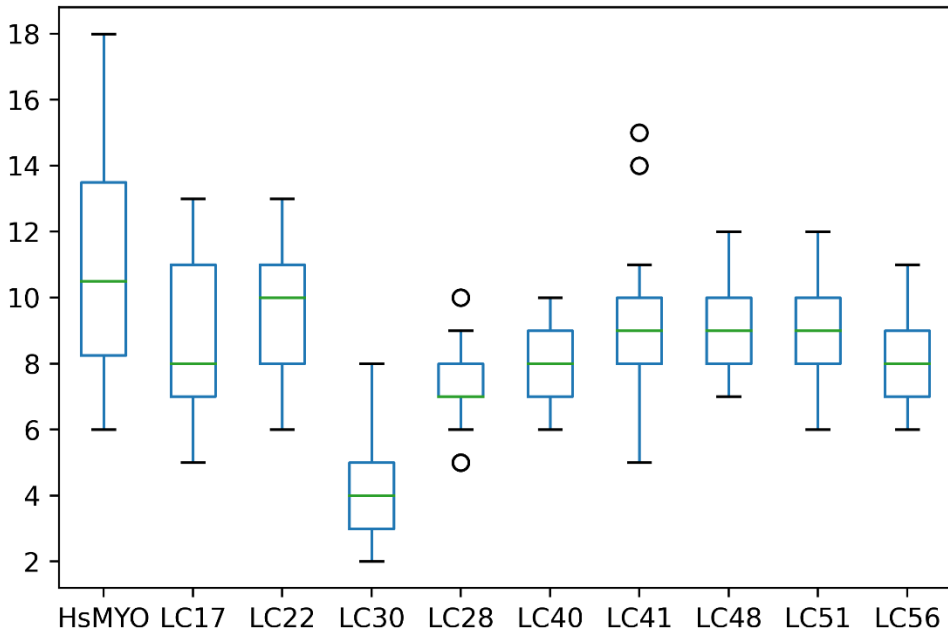
Figure 41: Double-blinded Stomatal Density Assays of Each Candidate and HsMYO Plants.

Stomatal density assays comparing the average number of stomata between each candidate and HsMYO plants. A one-way ANOVA among the groups yields a p-value < .0001. A Tukey-Kramer post hoc test reveals a statistically significant difference between HsMYO and LC30 plants. No other statistically significant difference was found. The fifth true leaf of five different plants from each condition were harvested as samples. Five different images from each sample were taken via bright-field microscopy, totaling 25 images per genotype. The HsMYO data for all stomatal density assays is the same because all images were captured in the same experimental set.

3. DISCUSSION

Overall, there were 15 different lines from the amiRNA forward genetic screen that were investigated in this thesis. The 15 amiRNA candidate mutant plants can be categorized into four different categories based on the results obtained from the CO_2 variable gas exchange assays and stomatal density assays. First, there were five candidate plants which responded to imposed shifts in CO_2 concentrations in a similar manner to the HsMYO control plants. These candidate plant lines were: LC17, LC48, LC51, LC56, and LC57. LC17 was a line with a predicted downregulated receptor-like protein kinase, LC48 plants had a downregulated Sec14p-like Phosphatidylinositol transfer family protein, LC51 had a silenced tRNAse Z4 protein, LC56 was a plant line with an amiRNA predicted to downregulate transcription factor jumonji proteins, and LC57 was a TRAF-like family protein targeting amiRNA line. The CO_2-mediated stomatal conductance was generally consistent with the HsMYO plants at ambient, low, and high CO_2 concentrations. Although the stomatal densities varied slightly among the amiRNA lines, none of these 5 lines had a statistically significant difference in terms of stomatal density when compared to the wild-type control. As there was no variation observed in CO_2-mediated stomatal conductance between the five aforementioned amiRNA lines and HsMYO control plants, it is highly unlikely the respective downregulated genes play a role in CO_2 signaling in plants. Consequently, these amiRNA lines will not be investigated further in any future experiments involving the more promising candidate lines from the forward genetic screen.

Second, there were two candidate plants with amiRNAs that targeted ribosomal proteins: LC42 and LC43. LC42 was a candidate plant line with a silenced 40S Ribosomal S19 Family protein while LC43 plants were a 40S Ribosomal S26e family protein targeting amiRNA line.

LC42 plants had a heavily affected response and LC43 plants had a mildly affected response in stomatal conductance from imposed shifts in CO_2 concentration. Both candidate plant lines had a statistically significant difference in stomatal density compared to the control plant lines. Importantly, ribosomes are present in all cells, not just guard cells, and are heavily involved in protein synthesis throughout the plant. It has been found that although specific ribosome protein genes may specialize into certain functions, ribosomes as a whole are widely heterogenous and regulate many different functions in plants (Martinez-Seidel et al., 2020). Thus, even though these preliminary data show promising results for the two ribosomal targeting amiRNA lines regarding CO_2-mediated stomatal conductance, it is likely the results are in part due to other vital processes being disturbed from ribosomal downregulation. Consequently, these amiRNA lines will not be investigated further in any future experiments involving the more promising candidate lines from the forward genetic screen.

Next, there were two candidate plants which had a mildly affected response in stomatal conductance from imposed shifts in CO_2 concentration, LC22 and LC40. LC22 was a candidate plant line with predicted targets of silenced formin gene homologs and LC40 plant lines carry an amiRNA that was predicted to downregulate F-box protein homologs. At ambient CO_2 conditions, both lines had a slightly reduced stomatal conductance compared to HsMYO plants. After low CO_2 exposure, LC22 plants responded slowly compared to control plants, but LC40 plants responded at a speed similar to the control plants. With high CO_2 exposure, LC22 plants responded at a speed similar to the control plants while LC40 plants responded slowly. LC22 plants had a similar stomatal density compared to the control, while there was a statistically significant reduction in number of stomata in LC40 plants comparted to control plants. While the results from these two candidate lines show moderate effects in terms of CO_2-mediated stomatal

conductance, the data was not striking enough for these lines to be a top priority. Eventually, these lines will be investigated in future experiments, but for initial future experiments they will not be studied.

Finally, there were six amiRNA candidate plants with interesting results, either from the stomatal density data or stomatal conductance data. These six plants were: LC30, LC28, LC41, LC35, LC71, and LC72. LC30 plants were a leucine-rich repeat protein targeting amiRNA line, LC28 were a candidate plant line with downregulated nascent polypeptide-associated complex subunit alpha-like protein (NACA-like protein) homologs, LC41 was an amiRNA line predicted to downregulate F-Box mRNAs, LC35, a plant line with an amiRNA predicted to downregulate transcription factor jumonji proteins, LC71 plants were predicted to down regulate phototropic-responsive NPH3 family proteins, and LC72 plants had an amiRNA predicted to silence tetratricopeptide repeat (TPR)-like superfamily protein homologs. LC28, LC41, LC35, LC71, and LC72 plants all had heavily affected responses to CO_2-mediated stomatal conductance. The stomatal densities differed among the different amiRNA lines, but generally there was no major difference in number of stomata between the candidates and the HsMYO control. An ANOVA analysis found no statistically significant differences in number of stomata between the candidates and the HsMYO control. Meanwhile, LC30 plants showed a highly shifted stomatal conductance response curve to CO_2 that may be explained by the large difference in number of stomata compared to control plants. An ANOVA analysis showed LC30 had a statistically significant difference in number of stomata when compared to the control plants. Due to these noteworthy results, we have decided to focus on these six amiRNA candidates for further characterization and experimentation.

One of the targeted LRR family protein loci in LC30 is predicted to have a secondary interaction with known CO_2 signaling component OST1 (Figure 9A). However, OST1 is shown to be involved in CO_2-mediated stomatal conductance rather than a stomatal development phenotype as seen in LC30 (Xue et al., 2011). Thus, the relationship between the LRR protein in LC30 and OST1 is not likely to play a role in the developmental phenotype. Importantly, LRR-like kinases have been previously shown to be involved in stomatal development, such as stomatal symmetry (Keerthisinghe et al., 2015). More research must be conducted at the early stages of stomatal formation to understand the effects the downregulated LRR proteins in LC30 have on stomatal development.

For LC28, it is possible the downregulated NACA-like protein homologs play a role in CO_2 signaling. These candidate plants have a CO_2-mediated stomatal response similar to when known CO_2 signaling genes, such as ht1, are mutated in plants (Hashimoto et al., 2006). NAC1, a specific nascent polypeptide-associated complex protein, has been shown to interact with mitogen activated kinases (MAPK; Wang et al., 2020). Further, there are two MAPKs that are known to be associated in CO_2 signaling in *A. thaliana*, MPK4 and MPK12, so it is possible the silenced NACA-like protein in LC28 interacts with these MAPKs (Tõldsepp et al., 2018). Thus, protein-protein interaction experiments can be conducted in the future to ascertain the relationship between the NACA-like protein homologs and MAPKs in *A. thaliana.*

One of the targeted F-box protein loci in LC41 is predicted to have a primary interaction with STP4 and a secondary interaction with known CO_2 signaling component AtPIP2; 1 (Figure 18). LC41 plants were shown to have a delayed stomatal response to both low and high levels of CO_2. Sugar Transporter Protein 1 and 4 double mutants (*stp1stp4)* were shown to have a reduced light-induced stomatal opening due to a lack of glucose uptake in guard cells (Flütsch et al.,

2020). However, time course stomatal conductance assays of imposed shifts in $[CO_2]$ were not performed. It is possible the limited glucose supply in guard cells prevents immediate stomatal response to shifts in $[CO_2]$. Furthermore, the silenced F-box proteins in LC41 amiRNA lines may lead to limited activation of the sugar transporters in guard cells and lead to a phenotype similar to the one seen in *stp1stp4*. Additionally, a different targeted F-box protein loci in LC41 is predicted to interact with a secondary interaction with known CO_2 signaling component TPK1, shown to be involved in stomatal closure (Figure 38; Isner et al., 2018). The downregulation of the F-box proteins in LC41 may have led to the phenotype seen in LC41 plants after 120 minutes of high CO_2 treatment (Figure 15). Further tests will be necessary to discover the relationship between the F-box protein, STP4, TPK1, and CO_2.

Jumonji proteins are known to be involved in plant development and response through chromatin modifications (Yamaguchi, 2021). The targeted jumonji proteins in LC35 may therefore play a role in responding to changes in the environment regarding shifts in $[CO_2]$. Protein-protein interaction experiments may be performed to determine the importance of jumonji proteins in CO_2-mediated stomatal conductance.

There are a few ways the NPH3 family proteins in LC71 may be affecting CO_2-mediated stomatal conductance. NPH3 proteins are known to be necessary for phototropism, or plant growth response to blue light (Motchoulski and Liscum, 1999). Importantly, there has recently been a link shown between blue light and CO_2 signaling through CBC1/2, a kinase involved at the crossroads of both pathways (Hiyama et al., 2017). Thus, the amiRNA targets of LC71 may also be involved with CBC1/2, but how is uncertain. One of the targeted loci in LC71 was also predicted to interact with multiple CO_2 signaling components: BCA1, BCA4, BIG, and TPK1, albeit through intermediate interactor UBQ3. Although ubiquitination is normally seen in plants

56

as a marker for protein degradation, it has been shown to also act as a marker for protein regulation in signaling pathways of plant immunity (Zhou and Zeng, 2017). Future experiments involving light and possibly UBQ3 should be tested to investigate the role of NPH3 family proteins in LC71 and CO_2 signaling.

Not much is known about TPR proteins and the TPR-like protein homologs downregulated in LC72 in regards to CO_2 signaling, but TPR proteins have been shown to be involved in other signaling pathways in *A. thaliana,* such as ABA signal transduction (Rosado et al., 2006). There are a few genetic components such as OST1 and SLAC1 which are involved in both ABA signaling and CO_2 signaling, so is possible for TPR proteins to also be at an intersection of pathways (Xue et al., 2011; Geiger et al., 2009). Studies regarding drought stress and CO_2 signaling must be conducted to ascertain the effect of the silenced TPR-like protein homologs in LC72.

One major limitation of these data is that the transformation event itself may be the cause of the phenotype seen in the stomatal conductance graphs. As the insertion event is random, the amiRNA may be inserted into a key CO_2 signaling pathway gene or the promoter region of an important CO_2 signaling gene, thus impacting CO_2-mediated stomatal conductance and causing the phenotype seen. In these cases, although CO_2-mediated stomatal conductance is affected in these amiRNA lines, the downregulation of the specific amiRNA is not necessarily the reason but rather the affected expression of a known CO_2 signaling gene. Additionally, genome wide sequencing was not completed to determine the location of amiRNA insertion, so it is unknown exactly where the amiRNA is inserted.

Ultimately, there are a number of genes that are seemingly involved in CO_2-mediated stomatal conductance, but further experimentation is necessary. Confirmation of these stomatal

movement and stomatal development mutants must be completed to verify the robustness of the phenotypes. Retransformations of wild-type Col0 with the same amiRNAs as the original mutants and T-DNA insertion crosses can be grown to support the results found in this thesis. Retransformations of Col0 (wild type) plants with the same amiRNA as the initial candidate plants will lead to a new transformation event. This will likely insert the amiRNA in a different location within the genome compared to the initial amiRNA screen, allowing one to determine if the stomatal response of the plant is due to the insertion event itself limiting important gene transcription or the downregulation of the targeted genes resulting in the phenotype.

Currently, retransformations of wild-type Col0 of the most promising candidates are being grown and are in the T1 generation. Current and future generations of the retransformations will be grown on ½ Murashige and Skoog basal medium (MS) plates with 15 µg/mL BASTA to ensure the retransformation event was successful and select against seeds without BASTA resistance. Infrared thermal imaging after low CO_2 treatment will be performed on the next generation (T2) plants to verify the robustness of the amiRNA retransformation event, and the strongest lines will be selected to grow up for future experiments. The conditions will follow the initial primary screen, where many seedlings were grown in one medium 4-inch pot and pretreated with 150 ppm CO_2 for 2 hours before infrared thermal imaging. In the subsequent T3 generation, infrared thermal imaging after low CO_2 treatment will be performed to verify the robustness of each line selected in the previous infrared thermal imaging screen, and the strongest lines will be used for gas exchange experiments and stomatal density assays. The conditions will follow the secondary confirmation screen where two candidate plants were grown with a cold control HsMYO plant and hot control *ht1-2* plant to three weeks and treated with 150 ppm CO_2 for 2 hours before infrared thermal imaging.

Furthermore, different types of mutant plants can also be tested to confirm the stomatal conductance phenotypes seen in the amiRNA candidates such as T-DNA insertion mutants, which are another mutation commonly used in plant biology to knockdown genes and are easily designable through online resources (O'Malley et al., 2015). Because T-DNA insertions only target one specific locus, crosses between multiple T-DNA insertion mutants will be required to match the loci targeted in the amiRNA candidates. For example, candidate LC71 has two loci targeted, AT1G30440 and AT4G37590, so the T-DNA insertion line targeting AT1G30440 and the T-DNA insertion line targeting AT4G37590 will need to be crossed and future generation seeds verified to be homozygous for both genes (Table 1). Once this is complete, one can conduct CO_2-mediated stomatal conductance assays and stomatal density assays with these mutant plants to verify the results obtained from the candidate plants from the amiRNA screen.

In conclusion, an amiRNA forward genetic screen was performed to uncover new mutants involved in CO_2-mediated stomatal signaling in *Arabidopsis thaliana*. 75 initial mutants were identified in the primary thermal imaging screen and 39 putative mutants were isolated in the secondary confirmation thermal imaging screen (Swink, K. 2021). From the 39 putative mutants, I report six promising amiRNA candidates to be studied further for future experimentation. Five of these candidates displayed an affected CO_2-mediated stomatal conductance phenotype, which were LC28, a candidate plant line with downregulated nascent polypeptide-associated complex subunit alpha-like protein (NACA-like protein) homologs, LC41, an amiRNA line predicted to downregulate F-Box mRNAs, LC35, a plant line with an amiRNA predicted to downregulate transcription factor jumonji proteins, LC71, plants predicted to down regulate phototropic-responsive NPH3 family proteins, and LC72, plants with an amiRNA predicted to silence tetratricopeptide repeat (TPR)-like superfamily protein homologs.

The sixth candidate, LC30, was a leucine-rich repeat protein targeting amiRNA line and reportedly showed a stomatal development phenotype. As of now, it is still unknown how the promising candidates and their respective amiRNA loci targets fit into the currently accepted literature for CO_2 signaling in *A. thaliana.* Future experiments such as retransformations of Col0 wild type plants and T-DNA crosses of the targeted loci in the amiRNA candidates will provide further knowledge on the targeted loci and may verify the robustness of these candidates' phenotypes.

Table 1: Table of characterized amiRNA candidates in this thesis identified through a high-throughput loss of function genetic screen in low CO2 conditions. Leftmost column is the numbering system used to label each identified mutant and is used throughout this thesis. Sequencing data of the amiRNA, predicted protein class, loci, and status of re-transformation shown in latter columns.

Code	amiRNA	Protein class of predicted target	Locus silenced	Col0 re-transformation
LC17	TCAAGAGCGGCACTCGGACTG	Receptor-like protein kinase related	AT3G21910 AT3G21940 AT3G21960 AT3G22010	
LC22	TCCAAACAGTGGCGCGATCTA	Formin homolog	AT3G05470 AT5G67470	
LC27	TGTAAATGTTCAAGGTTCCGA	Leucine-rich repeat family protein	AT3G43740.1 AT3G43740.2 AT5G21090.1	T1 Lines Growing
LC28	TATTTAGGTGGTAAGTTCCAG	Nascent polypeptide-associated complex subunit alpha-like protein	AT3G12390 AT5G13850	T1 Lines Growing
LC30	TGTAAATGTTCAAGGTTCCGA	Leucine-rich repeat family protein	AT3G43740.1 AT3G43740.2 AT5G21090.1	T1 Lines Growing
LC33	TGTAAATGTTCAAGGTTCCGA	Leucine-rich repeat family protein	AT3G43740.1 AT3G43740.2 AT5G21090.1	T1 Lines Growing
LC35	TTCAACATGCCAGGCAAACAT	Transcription factor jumonji (jmj) family protein / zinc finger (C5HC2 type) family protein	AT3G48430 AT5G04240 AT5G46910	T1 Lines Growing

Table 1: Table of characterized amiRNA candidates in this thesis identified through a high-throughput loss of function genetic screen in low CO2 conditions, Continued"

LC40	TAATGTCGCACCTTTTAGCAC	F-box protein	AT1G30200.1 AT5G46170.1	T1 Lines Growing
LC41	TGAGTAATCATAAATGGCCTC	F-box protein	AT1G66290 AT1G66300 AT1G66310 AT1G66320 AT1G66640 AT1G78750 AT1G78840 AT4G13985	T1 Lines Growing
LC42	TAAGCGCATCGAGATCGGCAC	Ribosomal protein S19 family protein	AT1G33850 AT5G09490 AT5G09510 AT5G43640	
LC43	TGGAACGGACTCTTACCACGT	Ribosomal protein S26e family protein	AT2G40590 AT3G56340	T1 Lines Growing
LC48	TCATCGAGGTTTTGAGGCTG	Sec14p-like phosphatidylinositol transfer family protein	AT3G23960.1 AT1G19650.2 AT1G19650.1 AT1G19650.3 AT1G70500.1 AT1G61060.1 AT1G33010.1	
LC51	TATGTATAAGAACTGTTGCAC	tRNAse Z4	AT1G52160 AT3G16260	
LC56	TTCAACATGCCAGGCAAACAT	Transcription factor jumonji (jmj) family protein / zinc finger (C5HC2 type) family protein	AT3G48430 AT5G04240	
LC57	TTTGGAGGACGTTCTCGCCTA	TRAF-like family protein	AT3G20360 AT3G46190	
LC71	TAAAGAAGAGCACTTGTACAA	Phototropic-responsive NPH3 family protein	AT1G30440 AT4G37590	T1 Lines Growing
LC72	TATACATGTCTACGGGAGCTC	Tetratricopeptide repeat (TPR)-like superfamily protein	AT1G04840 AT1G31430	T1 Lines Growing

4. METHODS

Arabidopsis thaliana Growth

The model organism used in this paper was *Arabidopsis thaliana.* All *A. thaliana* lines were grown on ½ Murashige and Skoog basal medium (MS) plates with 15 µg/mL BASTA (Glufosinate-ammonium) added. The lines used in this project were the control line, named HsMYO, and the amiRNA candidate lines isolated from the previously mentioned forward genetic screen (Swink, K. 2021). HsMYO plants were used as the control in this project since they have an inserted amiRNA targeting the human myosin 2 gene and no targets in *A. thaliana* (Hauser et al., 2013). First, *A. thaliana* seeds were sterilized for 15 minutes with a 50% bleach sterilization solution. The seeds were then moved to a sterile flow hood before being washed 3 times with alternating sterile ultrapure water and 100% ethanol to remove excess sterilization solution. After the seeds were fully dried, the seeds were added to ½ MS plates and then sealed with micropore tape. Each plate contained at least 15 HsMYO seeds and 15 amiRNA candidate seeds for each line. The plates were incubated in a cold room at 4°C for 72 hours for cold temperature stratification, which is necessary to break seed dormancy and synchronize seed germination among the different lines.

The plates were then moved to a growth room with a 16h light/8h dark cycle at 21°C. The seedlings were grown on the ½ MS plates until the first true leaves of the seedlings began to sprout, and the seedlings were then carefully moved to individual 2-inch pots of soil. The soil used was Professional Growing Mix Sun Gro soil. The soil was autoclaved and moistened with deionized water and fertilizer to aid with growth conditions. Trays with the individual 2-inch pots were then covered with a high plastic dome to keep humidity consistent and moved to growth chambers with a 16h light/8h dark cycle at 21°C. Trays were monitored consistently and regularly watered to provide optimal growth conditions.

Thermal Imaging

Representative 3-week-old plants for each genotype were used in this report for infrared thermal imaging. Infrared thermal images were taken at ambient CO_2 conditions (~415 ppm) without any incubation at low CO_2 before imaging. Infrared images were taken with a "FLIR T650sc series thermal imaging camera outfitted with a 25° lens" (Swink, K. 2021). Brightfield images were taken with a Canon EOS camera immediately after the thermal imaging camera with the same environmental conditions to note for any phenotypical differences. Importantly, note that these conditions are not the same screening conditions as the primary screen and confirmation screen, which utilized incubation of plants at low CO_2 (150 ppm) for 2 hours before infrared thermal images were taken. FLIR Tools were used for temperature analysis. To estimate the whole plant temperature for each plant, the temperature of each individual leaf was recorded and averaged.

Gas Exchange Assay

Representative 5-6-week-old plants for each genotype were used in this report to measure stomatal conductance (gs) through gas exchange analysis. Plants were grown to 5-6 weeks old in individual 2-inch pots and a single, healthy leaf was inserted into a LiCOR 6400XT machine. Leaves were incubated at optimal conditions of 21°C, blue light intensity of 150 μmol s^{-1} m^{-2} and flow rate of 500 μmol s^{-1} programmed in the LiCOR machine for 60 minutes. Silica beads were used to keep the leaves at ~65% relative humidity. After equilibration, a standard program started and recorded stomatal conductance values. For all experiments, the leaves were exposed to ambient CO_2 (400 ppm) for 30 minutes, low CO_2 (100 ppm) for 45 minutes, and high CO_2

(800 ppm) for 80 minutes. For each stomatal conductance graph in this report, the data represent the mean ± SEM of at least three leaves from independent distinct 5–6-week-old plants.

Stomatal Density Assay

The stomatal density assays performed in this project were double blinded, needing a total of 3 people to complete each assay. Person 1 harvested the fifth true leaf from 4–5-week-old plants of each genotype and incubated the leaves in 4 mL clarity solution in individual 15 mL centrifuge tubes for 24 hours. Person 1 would label each tube with a unique number that corresponds to the genotype of the harvested leaf. The clarity solution was created from a ratio of 1 acetic acid to 7 100% ethanol and removed the chlorophyll from the leaves and allowed for clearer imaging on a microscope. Person 2 would then take the numbered tubes and label them in a personal code for the first blind in the assay. Person 2 would not know the corresponding genotype for each tube.

Once the leaves were clarified for 24 hours, the blinded tubes would be given to Person 3 for microscopy. Person 3 would not know the order of the tubes or the corresponding genotype for each tube. The leaves were washed twice in deionized water to remove excess clarity solution and then incubated in 1M KOH for 15 minutes to soften the leaf. Each leaf was then moved to an individual microscope slide, abaxial side up. 75 µL of deionized water was added onto the microscope slide to allow for light to pass through the leaf sample. A microscope cover slip was then gently placed on top of the leaf. DIC microscopy was performed at 40X magnification with a "Nikon Eclipse TS100 microscope camera and the Sharpcap 3.1 program" (Swink, K. 2021). Five images of each leaf sample were taken in different spots. At least 5 samples of each genotype were harvested to total a minimum of 25 images per genotype. After microscopy, the

blinded images were given to Person 1 to count cells. Once cell counting was complete, the

samples were unblinded by Person 2 and Person 3 through their personal codes for data analysis.

Excel was used to "plot the data in box-whisker graphs and run a paired two-tailed t-test with

Welch's correction for all candidates with WT" (amiRNA-HsMYO, Swink, K. 2021).

Interactome via ePlant

  Interactomes were generated via ePlant from the University of Toronto browser for each

locus targeted by an amiRNA (Table 1, Waese et al., 2017). The link to the ePlant browser can

be found here: https://bar.utoronto.ca/eplant/. All amiRNA gene targets were searched and

predicted interactomes were generated through published datasets and databases. Per Swink, K.

2021, the datasets used include "Biomolecular Interaction Network Database (BIND) (Popescu

et al., 2007; Popescu et al., 2009), Arabidopsis Interactome (Arabidopsis Interactome Mapping

Consortium, 2011), Membrane protein INteractome Database (MIND) (Frommer et al., 2009),

and BioGRID (Stark et al., 2006)". The viewer was built with CytoscapeJS using Javascript

(Waese et al., 2017).

Interactome via Python

  Interactomes were generated via a personally written Python code to search through

published datasets not utilized in the ePlant browser for each locus targeted by an amiRNA

(Table 1). Although the ePlant browser contains many datasets and databases, there are newer

papers which were not used to generate interactomes in ePlant. Additionally, a newer version of

the BioGRID dataset was released, but was not yet been updated in the ePlant browser, so this

Python script allowed for more interactions to be found. These interactomes created via Python

were meant to act as a supplement to the interactomes generated via ePlant, and some of these

interactomes overlap with interactions included in the interactomes from the ePlant browser.

Interactomes which contained the exact same interactions from ePlant but generated in Python

were not included in this thesis to reduce redundancy.

```python
import pandas as pd
import matplotlib.pyplot as plt
import networkx as nx


biogrid_data = pd.read_csv("biogrid1.txt", delimiter= "\t")

annotations = pd.read_csv("Annotations_40s.csv")
gene_sheet = annotations.iloc[25:81,1:3]


genes = list(gene_sheet["Gene (AT)"])

gene_dict = gene_sheet.set_index('Gene (AT)').T.to_dict('list')

gene_set = set(gene_sheet["Gene (AT)"])


biogrid_data_select = biogrid_data.iloc[:, 5:7]
print(biogrid_data_select.head())
for i, gene in enumerate(genes):
    biogrid_data_geneA = biogrid_data_select[biogrid_data_select['Systematic Name Interactor A'].isin([gene])]
    biogrid_data_geneB = biogrid_data_select[biogrid_data_select['Systematic Name Interactor B'].isin([gene])]
    combined_data = pd.concat([biogrid_data_geneA, biogrid_data_geneB])

    if gene in gene_dict.keys():
        label = gene.replace(gene, gene + str(gene_dict[gene]))
        genes[i] = label

    edgelist = combined_data.values.tolist()
    for j, list in enumerate(edgelist):
        for k, edge in enumerate(list):
            if edge in gene_dict.keys():
                label_2= edge.replace(edge, edge + str(gene_dict[edge]))
                list[k] = label_2
```

Figure 42: Python Script to Generate Interactomes.

Python script used to generate predictive interaction networks between amiRNA candidates and known CO_2 signaling components. The script was mainly built using NetworkX, a Python package used to create networks. Necessary files to run the script include: biogrid1.txt – downloadable text file of *Arabidopsis thaliana* data from BioGRID and Annotations_40s.csv – csv or excel file which converts AGI numbers found on BioGRID file to common gene names and amiRNA candidate number. Creation of nodes is also necessary to run script properly.

5. REFERENCES

Bellati, J., Champeyroux, C., Hem, S., Rofidal, V., Krouk, G., Maurel, C., & Santoni, V. (2016). Novel Aquaporin Regulatory Mechanisms Revealed by Interactomics. *Molecular & cellular proteomics : MCP*, *15*(11), 3473–3487. https://doi.org/10.1074/mcp.M116.060087

Chen, T., Wu, H., Wu, J., Fan, X., Li, X., & Lin, Y. (2017). Absence of *Os β CA1* causes a CO_2 deficit and affects leaf photosynthesis and the stomatal response to CO_2 in rice. *The Plant Journal*, *90*(2), 344–357. https://doi.org/10.1111/tpj.13497

Dubeaux, Guillaume. (2019). *amiRNA Forward Genetic Screen [Unpublished Data]*

Engineer, C. B., Hashimoto-Sugimoto, M., Negi, J., Israelsson-Nordström, M., Azoulay-Shemer, T., Rappel, W.-J., Iba, K., & Schroeder, J. I. (2016). CO 2 Sensing and CO 2 Regulation of Stomatal Conductance: Advances and Open Questions. *Trends in Plant Science*, *21*(1), 16–30. https://doi.org/10.1016/j.tplants.2015.08.014

Flütsch, S., Nigro, A., Conci, F., Fajkus, J., Thalmann, M., Trtílek, M., Panzarová, K., & Santelia, D. (2020). Glucose uptake to guard cells via STP transporters provides carbon sources for stomatal opening and plant growth. *EMBO Reports*, *21*(8). https://doi.org/10.15252/embr.201949719

Geiger, D., Scherzer, S., Mumm, P., Stange, A., Marten, I., Bauer, H., Ache, P., Matschi, S., Liese, A., Al-Rasheid, K. A., Romeis, T., & Hedrich, R. (2009). Activity of guard cell anion channel SLAC1 is controlled by drought-stress signaling kinase-phosphatase pair. Proceedings of the National Academy of Sciences of the United States of America, 106(50), 21425–21430. https://doi.org/10.1073/pnas.0912021106

Hashimoto, M., Negi, J., Young, J., Israelsson, M., Schroeder, J. I., & Iba, K. (2006). Arabidopsis HT1 kinase controls stomatal movements in response to CO2. *Nature Cell Biology*, *8*(4), 391–397. https://doi.org/10.1038/ncb1387

Hauser, F., Ceciliato, P. H. O., Lin, Y.-C., Guo, D., Gregerson, J. D., Abbasi, N., Youhanna, D., Park, J., Dubeaux, G., Shani, E., Poomchongkho, N., & Schroeder, J. I. (2019). A seed resource for screening functionally redundant genes and isolation of new mutants impaired in CO2 and ABA responses. *Journal of Experimental Botany*. https://doi.org/10.1093/jxb/ery363

Hauser, F., Chen, W., Deinlein, U., Chang, K., Ossowski, S., Fitz, J., Hannon, G. J., & Schroeder, J. I. (2013). A genomic-scale artificial microRNA library as a tool to investigate the functionally redundant gene space in Arabidopsis. *The Plant cell*, *25*(8), 2848–2863. https://doi.org/10.1105/tpc.113.112805

Hiyama, A., Takemiya, A., Munemasa, S., Okuma, E., Sugiyama, N., Tada, Y., Murata, Y., & Shimazaki, K. (2017). Blue light and CO2 signals converge to regulate light-induced stomatal opening. *Nature Communications*, *8*(1), 1284. https://doi.org/10.1038/s41467-017-01237-5

Höök, M., & Tang, X. (2013). Depletion of fossil fuels and anthropogenic climate change—A review. *Energy Policy*, *52*, 797–809. https://doi.org/10.1016/j.enpol.2012.10.046

Hõrak, H., Sierla, M., Tõldsepp, K., Wang, C., Wang, Y.-S., Nuhkat, M., Valk, E., Pechter, P., Merilo, E., Salojärvi, J., Overmyer, K., Loog, M., Broché, M., Schroeder, J. I., Kangasjärvi, J., & Kollist, H. (2016). A Dominant Mutation in the HT1 Kinase Uncovers Roles of MAP Kinases and GHR1 in CO$_2$-Induced Stomatal Closure. *The Plant Cell*, *28*(10), 2493–2509. https://doi.org/10.1105/tpc.16.00131

Howe, J. P. (2015). This Is Nature; This Is Un-Nature: Reading the Keeling Curve. *Environmental History*, *20*(2), 286–293. https://doi.org/10.1093/envhis/emv005

Hsu, P. K., Takahashi, Y., Munemasa, S., Merilo, E., Laanemets, K., Waadt, R., Pater, D., Kollist, H., & Schroeder, J. I. (2018). Abscisic acid-independent stomatal CO2 signal transduction pathway and convergence of CO2 and ABA signaling downstream of OST1 kinase. *Proceedings of the National Academy of Sciences of the United States of America,* 115(42), E9971–E9980. https://doi.org/10.1073/pnas.1809204115

Hu, H., Rappel, W.-J., Occhipinti, R., Ries, A., Böhmer, M., You, L., Xiao, C., Engineer, C. B., Boron, W. F., & Schroeder, J. I. (2015). Distinct Cellular Locations of Carbonic Anhydrases Mediate Carbon Dioxide Control of Stomatal Movements. *Plant Physiology*, *169*(2), 1168–1178. https://doi.org/10.1104/pp.15.00646

Isner, J. C., Begum, A., Nuehse, T., Hetherington, A. M., & Maathuis, F. (2018). KIN7 Kinase Regulates the Vacuolar TPK1 K+ Channel during Stomatal Closure. Current biology : CB, 28(3), 466–472.e4. https://doi.org/10.1016/j.cub.2017.12.046

Jakobson, L., Vaahtera, L., Tõldsepp, K., Nuhkat, M., Wang, C., Wang, Y. S., Hõrak, H., Valk, E., Pechter, P., Sindarovska, Y., Tang, J., Xiao, C., Xu, Y., Gerst Talas, U., García-Sosa, A. T., Kangasjärvi, S., Maran, U., Remm, M., Roelfsema, M. R., Hu, H., … Broché, M. (2016). Natural Variation in Arabidopsis Cvi-0 Accession Reveals an Important Role of MPK12 in Guard Cell CO2 Signaling. *PLoS biology*, *14*(12), e2000322. https://doi.org/10.1371/journal.pbio.2000322

Kapilan, R., Vaziri, M. & Zwiazek, J.J. Regulation of aquaporins in plants under stress. *Biol Res* **51,** 4 (2018). https://doi.org/10.1186/s40659-018-0152-0

Keeling, C. D., Bacastow, R. B., & Bainbridge, A. E. (1976). Atmospheric carbon dioxide variations at Mauna Loa Observatory, Hawaii. *TELLUS,* 28(6): 538-51. https://doi.org/10.3402/tellusa.v28i6.11322

Keenan, T. F., Hollinger, D. Y., Bohrer, G., Dragoni, D., Munger, J. W., Schmid, H. P., & Richardson, A. D. (2013). Increase in forest water-use efficiency as atmospheric carbon dioxide concentrations rise. *Nature*, *499*(7458), 324–327. https://doi.org/10.1038/nature12291

Keerthisinghe, S., Nadeau, J. A., Lucas, J. R., Nakagawa, T., & Sack, F. D. (2015). The Arabidopsis leucine-rich repeat receptor-like kinase MUSTACHES enforces stomatal bilateral symmetry in Arabidopsis. The Plant journal : for cell and molecular biology, 81(5), 684–694. https://doi.org/10.1111/tpj.12757

Koornneef, M., & Meinke, D. (2010). The development of Arabidopsis as a model plant. *The Plant Journal*, *61*(6), 909–921. https://doi.org/10.1111/j.1365-313X.2009.04086.x

Marten, H., Hyun, T., Gomi, K., Seo, S., Hedrich, R., & Roelfsema, M. R. (2008). Silencing of NtMPK4 impairs CO-induced stomatal closure, activation of anion channels and cytosolic Casignals in Nicotiana tabacum guard cells. *The Plant Journal*, 55(4), 698–708. https://doi.org/10.1111/j.1365-313X.2008.03542.x

Martinez-Seidel, F., Beine-Golovchuk, O., Hsieh, Y. C., & Kopka, J. (2020). Systematic Review of Plant Ribosome Heterogeneity and Specialization. *Frontiers in plant science*, *11*, 948. https://doi.org/10.3389/fpls.2020.00948

Motchoulski, A., & Liscum, E. (1999). Arabidopsis NPH3: A NPH1 photoreceptor-interacting protein essential for phototropism. Science (New York, N.Y.), 286(5441), 961–964. https://doi.org/10.1126/science.286.5441.961

Negi, J., Matsuda, O., Nagasawa, T., Oba, Y., Takahashi, H., Kawai-Yamada, M., Uchimiya, H., Hashimoto, M., & Iba, K. (2008). CO2 regulator SLAC1 and its homologues are essential for anion homeostasis in plant cells. *Nature*, *452*(7186), 483–486. https://doi.org/10.1038/nature06720

O'Malley, R. C., Barragan, C. C., & Ecker, J. R. (2015). A user's guide to the Arabidopsis T-DNA insertion mutant collections. *Methods in molecular biology (Clifton, N.J.)*, *1284*, 323–342. https://doi.org/10.1007/978-1-4939-2444-8_16

Oughtred, R., Rust, J., Chang, C., Breitkreutz, B. J., Stark, C., Willems, A., Boucher, L., Leung, G., Kolas, N., Zhang, F., Dolma, S., Coulombe-Huntington, J., Chatr-Aryamontri, A., Dolinski, K., & Tyers, M. (2021). The BioGRID database: A comprehensive biomedical resource of curated protein, genetic, and chemical interactions. *Protein science : a publication of the Protein Society*, *30*(1), 187–200. https://doi.org/10.1002/pro.3978

Park, S. Y., Fung, P., Nishimura, N., Jensen, D. R., Fujii, H., Zhao, Y., Lumba, S., Santiago, J., Rodrigues, A., Chow, T. F., Alfred, S. E., Bonetta, D., Finkelstein, R., Provart, N. J., Desveaux, D., Rodriguez, P. L., McCourt, P., Zhu, J. K., Schroeder, J. I., Volkman, B. F., … Cutler, S. R. (2009). Abscisic acid inhibits type 2C protein phosphatases via the

PYR/PYL family of START proteins. *Science (New York, N.Y.)*, *324*(5930), 1068–1071. https://doi.org/10.1126/science.1173041

Rosado, A., Schapire, A. L., Bressan, R. A., Harfouche, A. L., Hasegawa, P. M., Valpuesta, V., & Botella, M. A. (2006). The Arabidopsis tetratricopeptide repeat-containing protein TTL1 is required for osmotic stress responses and abscisic acid sensitivity. Plant physiology, 142(3), 1113–1126. https://doi.org/10.1104/pp.106.085191

Schwab, R., Ossowski, S., Riester, M., Warthmann, N., & Weigel, D. (2006) Highly Specific Gene Silencing by Artifical MicroRNAs in Arabidopsis. *The Plant Cell, 18,* 1121-1133. https://doi.org/10.1105/tpc.105.039834

Swink, K. J. (2021). Elucidating Novel Factors in the Plant Guard Cell CO2 Signaling Pathway: A Complementary Forward Genetic Screen in Arabidopsis thaliana. *UC San Diego*. ProQuest ID: Swink_ucsd_0033M_20174. Merritt ID: ark:/13030/m5gv1cmb. Retrieved from https://escholarship.org/uc/item/5zj0r5wv

The Arabidopsis Genome Initiative (2000). Analysis of the genome sequence of the flowering plant Arabidopsis thaliana. *Nature*, *408*(6814), 796–815. https://doi.org/10.1038/35048692

Tõldsepp, K., Zhang, J., Takahashi, Y., Sindarovska, Y., Hõrak, H., Ceciliato, P., Koolmeister, K., Wang, Y. S., Vaahtera, L., Jakobson, L., Yeh, C. Y., Park, J., Brosche, M., Kollist, H., & Schroeder, J. I. (2018). Mitogen-activated protein kinases MPK4 and MPK12 are key components mediating CO2 -induced stomatal movements. The Plant journal : for cell and molecular biology, 96(5), 1018–1035. https://doi.org/10.1111/tpj.14087

Xue, S., Hu, H., Ries, A., Merilo, E., Kollist, H., & Schroeder, J. I. (2011). Central functions of bicarbonate in S-type anion channel activation and OST1 protein kinase in CO2 signal transduction in guard cell. *The EMBO journal*, 30(8), 1645–1658. https://doi.org/10.1038/emboj.2011.68.

Waese, J., Fan, J., Pasha, A., Yu, H., Fucile, G., Shi, R., Cumming, M., Kelley, L. A., Sternberg, M. J., Krishnakumar, V., Ferlanti, E., Miller, J., Town, C., Stuerzlinger, W., & Provart, N. J. (2017). ePlant: Visualizing and Exploring Multiple Levels of Data for Hypothesis Generation in Plant Biology. The Plant cell, 29(8), 1806–1821. https://doi.org/10.1105/tpc.17.00073

Wang, P., Wu, P., Huang, R., & Chung, K. (2020). The Role of a Nascent Polypeptide-Associated Complex Subunit Alpha in Siderophore Biosynthesis, Oxidative Stress Response, and Virulence in *Alternaria alternata. The American Phytopathological Society, 33(4)*. https://doi.org/10.1094/MPMI-11-19-0315-R

Yamaguchi N. (2021). Removal of H3K27me3 by JMJ Proteins Controls Plant Development and Environmental Responses in Arabidopsis. Frontiers in plant science, 12, 687416. https://doi.org/10.3389/fpls.2021.687416

Zhang, J., De-oliveira-Ceciliato, P., Takahashi, Y., Schulze, S., Dubeaux, G., Hauser, F., Azoulay-Shemer, T., Tõldsepp, K., Kollist, H., Rappel, W.-J., & Schroeder, J. I. (2018). Insights into the Molecular Mechanisms of CO2-Mediated Regulation of Stomatal Movements. *Current Biology*, *28*(23), R1356–R1363. https://doi.org/10.1016/j.cub.2018.10.015

Zhang, L., Takahashi, Y., Hsu, P. K., Kollist, H., Merilo, E., Krysan, P. J., & Schroeder, J. I. (2020). FRET kinase sensor development reveals SnRK2/OST1 activation by ABA but not by MeJA and high CO_2 during stomatal closure. *eLife*, *9*, e56351. https://doi.org/10.7554/eLife.56351

Zhou, B., & Zeng, L. (2017). Conventional and unconventional ubiquitination in plant immunity. *Molecular plant pathology*, *18*(9), 1313–1330. https://doi.org/10.1111/mpp.12521